AALBORG UNIVERSITET

OPTIMIZING OIL-WATER SEPARATION : A COMPARATIVE STUDY OF SYNTHETIC AND BIOLOGICAL COAGULANTS AND FLOCCULANTS WITH EMPHASIS ON EXTRACELLULAR POLYMERIC SUBSTANCES (EPS)

30 ECTS Master Thesis

Author:
Maria Magdalena Tuzikiewicz

SUPERVISORS :
Morten Lykkegaard Christensen
Gustav Simoni

AALBORG UNIVERSITET
Departament of Chemistry and Bioscience

June 2024
Page numbers: 46

Abstract

A significant amount of wastewater is created by the oil and gas sector, which is responsible for producing produced water (PW), which is an emulsion of oil-water. To reduce environmental impact, traditional treatment approaches including physical, chemical and biological treatments are used. Oily water treatment become a significant problem and is now an important topic among engineers when it comes to undoing the harm. Because of the molecular interactions and repulsive forces acting on the particles creating PW, it is really hard to perform the demulsifying operations and separate the substances. This study examines the effectiveness of several coagulants and flocculants, crucial for PW treatment processes. Cationic starch and EPS II obtained promising results and qualify as good synthetic flocculant substitutes. In the group of synthetic coagulants, ironic sulfate (PIX113) appeared as the most effective one. This study also looked at the order of substances added to separate oil emulsions. In the majority of $CaCl_2$ dosages, EPS II at pH 8 worked best when added first. However, the lowest turbidity results were obtained when $CaCl_2$ was added first, but only within the 450 – 1000 [µl] dosage of $CaCl_2$. These results imply that conducting more research within that area can increase the biocoagulants' capacity to replace the synthetic ones. The efficiency of EPS I and EPS II is strongly influenced by pH, which also affects zeta potential, particle size and viscosity. In a neutral/basic environment, both EPS I and EPS II accompanied by $CaCl_2$, performed at their best, with EPS II revealing the highest turbidity removal efficiency at pH 8. Fourier Transform Infrared Spectroscopy analysis exposed that EPS I and EPS II have comparable chemical compositions, despite distinct origin sources, indicating that they can be used compatibly as a coagulant. The significance of dosage, pH and coagulant sequencing was brought up to attention throughout this research. This study aims to contribute to more sustainable water treatment solutions.

Preface

This Master's thesis is submitted as a fulfillment of the Master's degree in Environmental Science at the Aalborg Universitet. The project has been carried out in the period from January 2024 to June 2024 and is rated to 30 ECTS.

Maria Turkiewicz

03.06.24

Table of Contents

Table of Figures

1. Introduction

Oil and gas industries are responsible for massive wastewater production as a side effect of the oil production processes. Produced water (PW) is a general term used to describe oil-water emulsions, which are a byproduct during oil and gas operations. It is estimated that oil and gas sector brings about 39,5 thousand m^3/day of produced water, whereas globally the PW production volume is estimated to be around 200 million barrels/per day. (Gul Zaman et al. 2021) PW is a mixture of inorganic and organic compounds, such as salts, metals, suspended particles, hydrocarbons and other supplements which are added during the production processes. Due to the high hazardous contaminants present in the side product water, it is crucial to take action to protect the environment. It is important to assess and incorporate feasible options for PW management and disposal into the design of the production (Anon 2007). Some traditional treatment techniques for produced water can minimize environmental harm, including physical, chemical and biological techniques (Gul Zaman et al. 2021).

A few million tonnes of oil from transportation activities is incorporated into the world's water supplies adding as a source of pollution daily. The first precaution to be taken is to establish limits on pollution sources to mitigate the harm. Hence, the International Convention for the Prevention of Pollution from the Ships, MARPOL was created to guide and control pollution from sea transport – ships, different kinds of vessels and operation platforms. MARPOL has set different waste categories concerning their origin and set requirements and orders for the management, storage and disposal of these. The MARPOL Annex I states regulations regarding oil discharge into the sea and sets limits present in discharged water. To reduce their negative effects on the maritime environment, ships must handle and dispose remains according to the regulations. Ports and coastal authorities are critical for this process since they should provide suitable waste treatment disposals and facilities (Anon n.d.-h). According to Marpol Annex I Part A (MARPOL Annex I n.d.) the oil tankers of 150gt and above and all ships of 400gt and above need to have an International Oil Pollution Prevention Certificate, which proves that demands in the Annexes are being followed. What is more, the document states that discharge of any oily mixtures into the sea from ships of 400gt and above is forbidden except if the conditions mentioned in that document are taken into consideration. One of them states that the oil content of the outflow does not exceed 15 ppm (MARPOL Annex I n.d.). OSPAR is another important organization which was created to help protect the marine environment, among others, by controlling oil discharges. It brings together 15 governments and the EU cooperate to protect North-East Atlantic (OSPAR Commission n.d.). According to the organization, the dispersed oil content in produced water, between the measured period of time, remained stable between 12,8mg/l and 14,6mg/l, which was below the limit value standard which is 30mg/l (OSPAR Commission 2016).

The second step, after prevention, is perceptive treatment of the already generated PW. Treating produced water is a challenge, where due to the lack of sustainability standards and treatment efficiency PW is still not safe for water reclamation purposes outside the energy sector (Scanlon et al. 2020). In wastewater treatment, we face many crucial processes, which in the end, bring us closer to reusing and disposing of water in the safest way possible. Wastewater treatment is a complicated process, which includes various steps, but in the end, safe water can be released into waterways, reused for many purposes, or even used again as a drinking water supply. The general scheme of industrial water treatment can be divided into three different stages – primary treatment which focuses on mechanical, physical and chemical methods, secondary treatment/purification step which focuses on chemical or biological methods and finally the treatment of the formed sludge (Renault et al. 2009). One of the biggest problems in the wastewater sector is the treatment of oily wastewater. It is usually composed of fats, oils, greases, organic and inorganic substances. Emulsions can be formed through addition of water, oil, gas, solids and depending on the fluid which becomes the continuous phase, they can be either oil-in-water (O/W) or water-in-oil (W/O) emulsions (Sousa, Pereira, and Matos 2022). They can be drawn apart by analyzing the forces that stabilize them. The O/W emulsions are stabilized by two acting forces – steric and electrostatic repulsion (Ushikubo and Cunha 2014). The O/W characterize themselves with an aqueous external phase (continuous part) and an oily internal phase. The produced water belongs to the oil-in-water (O/W) emulsions. When the emulsion is formed and stable, it is crucial to figure out how to reverse the process – demulsify the solution, with the best possible income, so the polluted water can be discharged safely (Sousa et al. 2022).

Crude bio-oil is a complex mixture liquid, produced by heating biomass to high temperatures (350-600 C) without the presence of oxygen. This process is known as pyrolysis, which is a thermochemical method of converting waste biomass into biofuels (syngas, char or bio-oil). The specific bio-oil characteristics are dependent on the type of biomass used. Temperature is the most important component that affects the properties of bio-oil, higher temperature results in improved bio-oil production (Anon n.d.-g). Even though the pyrolytic bio-oil is said to be an adequate diesel alternative, it carries a lot of disadvantages. *Typical bio-oil contains a significant amount of water (20-30%) and ash (0.04-0.24%) in its composition* (Ikura, Stanciulescu, and Hogan 2003). Due to that water content and the fact that it is originally produced from plants, it has lower calorific value than diesel, which makes it less efficient in case of usage. Bio-oil characterizes itself with having high viscosity. pH of the fluid is typically between 2,5 - 3,4. Due to the acids, alcohols, ketones, aldehydes and other high molecular weight groups, present in the bio-oil structure it is difficult to separate water from bio-oil (Ikura et al. 2003).

Some of the oil's compounds can lower the interfacial tension between fluids, which as a result will encourage the emulsification process (Sousa et al. 2022). Both, flocculation,

and coagulation are crucial wastewater processes that are included in chemical water treatment techniques. Those processes are usually applied in the primary purification stage but in some cases can also proceed in secondary treatment (Renault et al. 2009). In emulsions breaking, the first step to be taken is to encourage coagulation and flocculation processes among the droplets. The coagulation process will encourage the substance to destabilize, whereas the flocculation will promote destabilized particles to bind together, creating bigger flocks that are going to be easier to remove (Sousa et al. 2022).

2. Theory

Oil water emulsions often cause problems with operations and it might be difficult to break them up to return to the initial state (Sousa et al. 2022). Before being released into the natural environment, a significant portion of oily water produced needs to be separated. How to treat and recycle oily wastewater has become a critical topic among engineers, due to water scarcity problems, environmental pollution and degradation (Sousa et al. 2022). Oil water emulsions remain stable mostly due to molecular interactions between attractive forces between the particles. Repulsive forces, hydrophobic, van der Waals, electrostatic repulsive forces are the ones that mostly interfere with each other in keeping emulsion in balance (Scharnberg et al. 2023).

2.1 Emulsions stability

Oil-water emulsions stability can be affected by various aspects. In case of heavy oil industries, stability can be affected by the additional chemicals added to the oily water in order to enhance the EOR technologies, which are designed to recover oil that's left. Surfactant polymers added to oily water make emulsions more stable and it is difficult to separate liquids after that (Tian et al. 2022).

The dividing line between the external and internal phase of emulsion is called the interface. That's the place where particles from contiguous phases experience forces, that bind them together among their type. Combination of surface tension forces, intermolecular forces, acting surfactants or emulsifiers are binding and preventing the particles from separating. Hence, it makes it difficult to split an individual droplet into smaller particles. Those forces create interfacial tension, which keeps the two phases separate from mixing (Anon n.d.-e). Size of the particles present in the emulsion is important since it may affect the dynamic of the mixture. The gravity forces, as well as density between two fluids, will affect the particle distribution (Anon n.d.-e) (Shakeel, Farooq, and Chassagne 2020).

The primary cause of oil-water emulsions stability are emulsifiers, which are responsible for formation of stable film that can lower the interfacial tension and prevent merging of droplets. They usually consist of both hydrophilic and hydrophobic groups. The hydrophobic group consists most likely out of alkyl chains. Depending on the charges of the hydrophilic groups, we can categorize them into anionic, cationic, zwitterionic (with equal number of positively and negatively charged functional groups) and nonionic (neutral non-ionic state) (Tian et al. 2022).

2.2 Double Layer

Double-layer compression is a phenomenon where particles try to bind together while overcoming the force of repulsion (Owodunni and Ismail 2021a).

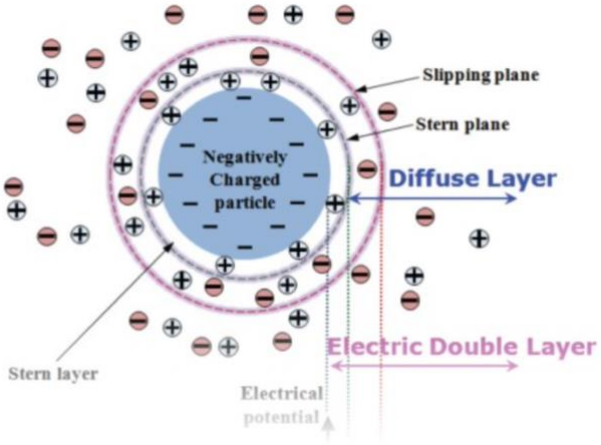

Figure 1 - Scheme of the Electric Double Layer, formed on a negatively charged particle (Rubenstein, Yin, and Frame 2015).

Figure 1 represents a negatively charged particle, which attracted positively charged ions to form a surrounding layer (Stern Layer). The next layer is a formation of both negatively and positively charged ions, since the positive ones are still drawn to the negatively charged colloid, where simultaneously, the stern layer is acting as a force back, pushing them away. This creates a Diffused Layer formed from counterions, that have a high concentration of positive ions near the colloidal surface, which decreases with distance, creating equality with negatively charged ions. The layer thickness depends on the solution type and concentration. The edge of this layer is called the slipping plate and it is a place where the stern layer and the diffused layer converge (Anon n.d.-c) (Rubenstein et al. 2015). The electrokinetic potential at the outer layer (slipping plane) is the Zeta Potential (Nisticò, Cesano, and Garello 2020).

2.2.1 Zeta Potential

An essential property in coagulation and flocculation is zeta potential. This indicator provides information on the charge of the particles and their ability to aggregate or to remain separate (Fatfat et al. 2023). The colloid carrying a charge will have an oppositely charged atmosphere, which results in electrical potential produced in the diffused layer. The zeta potential is the point connecting Stern and the diffuse layer. According to previous studies, particles that have zeta potentials greater than +30 mV or greater than -30 mV are typically viewed as stable. DLVO (Derjaguin, Landau, Verwey, and Overbek) theory states that *the stability of emulsions and colloids is a balance between the attractive van der Waals forces and the electrical repulsion because of the net surface charge* (Fatfat et al. 2023). Having that, the attraction forces will cause the emulsion droplets or colloids to clump if the zeta potential decline below a particular point. On the other hand, a stable system can be maintained by elevated zeta potential, neither positive nor negative. Extreme contradictory values of zeta potentials can cause substantial repulsive forces, then again having particles with similar electric charges can prevent aggregation and cause separation (Fatfat et al. 2023). In other words, the

fundamental concept of DLVO is that the van der Waals forces cause droplets to be drawn to one another. The larger the droplets, the harder it is to keep them apart, since the pull to one another increases with their radius. Small droplets are easily destroyed in the early phases of the emulsion formation, due to their close contact with particles of bigger radius (Anon n.d.-d).

2.2.2 Charge neutralization

The charge neutralization is directly related to the flocculation mechanism and its principles incorporate electric double layer and DLVO theory. Since the majority of scattered colloidal particles in the solution are charged, the electrostatic repulsion between them causes the system to stay in balance. When adding flocculants that carry opposite charges to the ones present in the system, the ionic strength is interrupted and the concentration of the double layers is intensified. Many oppositely charged ions are able to diffuse into the double layer, which results in a change of the particle charge. As a result, the zeta potential is reduced, which increases the probability of the collisions and bonding of the colloidal particles. This whole reaction causes the system to become unstable (Yang et al. 2016). The charge neutralization occurs around the isoelectric point (IEP), which is a point where no net electrical charge at a molecule is obtained. This point is highly dependent on the pH value of the colloidal environment and can change depending on gain or loss of protons (López-Maldonado, Oropeza-Guzmán, and Ochoa-Terán 2014).

2.3 Coagulation and Flocculation Mechanisms

The development of coagulation and flocculation technologies is crucial for practical applications such as wastewater treatment as well as scientific research. Retrieving oil-water using coagulation and flocculation mechanisms have great economic and environmental impact when it comes to current ecological systems (Kocaman and Yildiz 2023).

Coagulation process, by definition, *is a process whereby destabilization of a given suspension or solution is effected* (Bratby 2016) which states that the coagulant's role is to cause stability of a given unstable system. Coagulation process consists of using chemical coagulants which enable insoluble particles and dissolved organic matter to form larger particles. Chemicals such as aluminum or iron salts and organic polymers are added to neutralize the negative charge of the dispersed materials (Owodunni and Ismail 2021b) (Gernaey et al. 2017). Larger, denser flakes that are simpler to separate are created when a flocculation additive is added to the particles, bonding them together (Renault et al. 2009).

Flocculation is defined as *a process whereby destabilized particles, or particles formed as a result of destabilization, are induced to come together, make contact and thereby form larger agglomerates* (Bratby 2016). This process, contrary to coagulation, is a

process based on physical properties, which formate flocs from suspended particles present in the water. The process can be supported by high molecular weight polymers, which added to the colloidal particles create bridges that bind droplets together. Flocculation encourages binding of the particles, which results in creation of bigger flocs. Larger masses are easier to settle and be removed from the solution (Owodunni and Ismail 2021b) (Hogg 2012).

Flocculation process can be divided into two stages, the first one is due to perikinetic flocculation, which is a spontaneous phenomenon that is also known as Brownian movement. It starts as soon as destabilization occurs, molecules collide with each other which results in particles binding (Anon n.d.-b). Following that, the second stage of flocculation occurs which is known as orthokinetic flocculation, which results from generated liquid velocity gradients. Velocity gradients in a liquid medium behave in a way which causes the relative velocities of the particles to align, creating contact opportunities (Bratby 2016). The flocculation takes use of the desolubilization of the polymer, which functions as a net to entrap the emulsions.

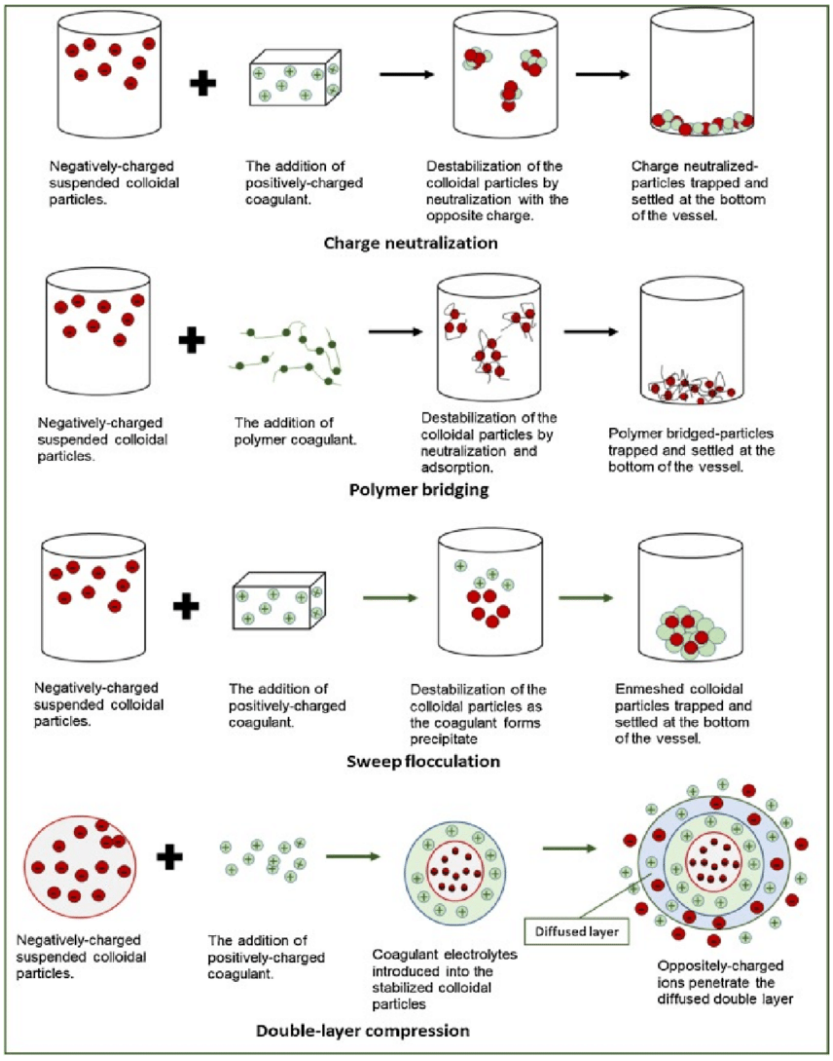

Figure 2 - Schematic diagram showing a depiction of the coagulant mechanism by adding different kinds of coagulants (Owodunni and Ismail 2021b)

Figure 2 represents different coagulation mechanisms after adding different kinds of coagulants. The coagulation and then flocculation processes are dependent on the particle charges and their ability to bond with each other. In all represented cases, negatively charged suspended colloidal particles are binding with positively charged substrates, which according to their structure, affect the formation and settling of the created flocs. According to the neutralization mechanism, the suspended particles are destabilized by being drawn to the oppositely charged electric ions. This action neutralizes their charges and causes a reduction or elimination of electrostatic repulsion. Next, flocculation takes place as the suspended colloids group together to create bigger flocs (Owodunni and Ismail 2021b).

The polymer bridging is represented as a second reaction in Figure 2, where high molecular weight polymers are added (in this case positively-charged) to the suspended colloidal particles (in this case negatively-charged) absorbing at the same time more than one particle. This can result in the production of large flocs. Due to their bigger size, these flocs have a lower surface area to mass ratio, which reduces the drag force acting on them. Consequently, gravitational forces dominate, leading to faster and more efficient settling at the bottom (Hogg 2012) (Owodunni and Ismail 2021c).

The last flocculation mechanism, represented in Figure 2, focuses on interactions with diffused double layer, which surrounds the colloidal particles. In the double-layer compression process, dose of electrolyte is added to the colloidal particles to enhance the flocculation process. The electrolyte can resist adhering to the colloid, due to the ability to remain impassive. Shift in anionic concentration causes the double layer, which is surrounding the colloid, to shrink. This results in lowering the repulsive energy barrier, when adequate compression of the layer is achieved. Thus, other forces (such as Vander wall forces) will override and the particles will join each other creating larger flocks (Zeta-Meter 1993) (Anon n.d.-c). The compression of the double layer is also called salting out the colloid.

When it comes to crude oil emulsions, demulsifiers typically work by weakening the interfacial film in an attempt to destabilize the solution. The interfacial behaviors of the materials interacting at the interface are important to reveal, to understand the whole process. In O/W emulsions, the anionic surfactants are demulsified with cationic demulsifiers hence, the charges are neutralized and ion pairs are formed. The anionic surfactants are set apart by cationic surfactants which enter in between fixed particles, forming ionic parts, causing the electrostatic repulsive force to decrease. With the weakened force, the separation of the O/W emulsion phases appears (Tian et al. 2022).

2.4 Parameters affecting coagulation/flocculation

Several environmental factors have an impact on the performance of the coagulation/flocculation processes. That includes pH, the dose of the

coagulant/flocculant, mixing rate, time, temperature, as well as physical properties - density and particle size of the additive. pH affects both, the activity of the coagulants/flocculants and the charge of particles which is why it is one of the crucial parameters for those processes (Badawi, Salama, and Mostafa 2023). . The isoelectric point can help determine the optimal pH range for flocculation (López-Maldonado et al. 2014).

When it comes to coagulants such as EPS, it is important to take into consideration the correlation between pH changes and EPS structural reactions to that. According to the study (Wang et al. 2012), after deep analysis of both protonated (state where the proton is added to the molecule) and deprotonated state (state where the proton is removed from the molecule), the lower pH value enhances the creation of more fixed and concentrated structure. The isoelectric point for that biopolymer is reached close to pH 4.8, where the highest flocculation effectiveness was obtained (Wang et al. 2012). The small particle size is linked to pH as well. At low pH (2), polymeric chains are more compact and not that willingly active. Whereas in a basic environment, the chains start to elongate and their structure is stretched out (Ofridam et al. n.d.).

In the coagulation/flocculation processes, the temperature can affect the charges of the particles, flocs setting, viscosity, and the rate at which particles collide with each other. According to (Zhang et al. 2018), under low temperatures (4°C – 17°C) the coagulation process is less efficient. Lower temperature decrease molecular movement due to reduction of kinetic energy of molecules. Since molecules have less energy to move around, the collision frequency between them decreases as well.

The mixing rate is an important factor that enhances the bonding of the added polymers with the colloid structure, which is a crucial factor for orthokinetic flocculation to occur. Nevertheless, created floc carries specific strength that depends on the bonds that were made during the aggregation process. When adding too much mixing and stress to the flocs surface, it might break the bonds that were made and destroy the whole created structure (Jiang 2015). Following the extensive, fast mixing, moderate mixing implies the start of the flocculation process. The surface charge of the particles decreases, as the electrical attraction to one another magnifies, which creates conditions for the flocculation process to occur. The flocs started to be seen since the particles start to group together. As the created flocs start to interact and bond with each other, creating larger masses, they begin to settle down at the bottom, starting the sedimentation process (Owodunni and Ismail 2021b).

The effectiveness of the flocculation can be enhanced by using more than one polymer to formulate the flocs. According to (Zeta-Meter 1993), firstly a highly charged positively charged polymer can be added, with the intention to neutralize the charge on the colloid, causing the formation of small flocs. Subsequently, a negatively charged polymer, carrying a high molecular weight, can bind the micro flocs together, creating larger

masses that can settle. The downfall of this procedure is that it is hard to estimate the ultimate charge balance and their acting forces. When polyelectrolytes alone can not smoothly destabilize the particles, it may be in favor of using an inorganic coagulant as a preliminary treatment in this process. This can also minimize the usage of cationic polymer, making the process more stable (Zeta-Meter 1993). Inorganic coagulants used as a preliminary treatment can remove some parts of suspended solids and organic matter, eliminating unnecessary disturbance in the further oil-water separation process. Flocculants can more clearly perform the oil-water separation without any disturbances, which leads to more predictable performance (Zeta-Meter 1993).

2.5 Introduction to Coagulants and Flocculants

At present, mineral additives including metal salts like polyaluminum chloride, ferric chloride aluminum sulfate, and synthetic polymers like polyacrylamide are commonly utilized as coagulants and flocculants. There is a need for change when it comes to currently used substances since the previously mentioned chemicals have number of negative effects on the environment. Rising concentration of metals in water, creation of unwanted toxic sludge, and dispersion of substances which may cause environmental hazards are only a few reasons for change (Renault et al. 2009). The research for new, environmentally friendly flocculants is ongoing. Biopolymers are discovered to be a promising solution as alternative coagulant and flocculant options. They are said to be low-cost products with eco-friendly nature trades, which makes them a great replacement (Renault et al. 2009). According to (Alazaiza et al. 2022), natural coagulants successfully treat wastewater, with low turbidity results oscillating between 50 to 500 NTU. Very promising results are given by moringa oleifera seed, cactus, starch, and chitosan (Lamanna et al. 2023).

The whole process goes as follows – coagulants such as, aluminum sulfate, ferric chloride, polyaluminium chloride, neutralize the charge on the particles, whereas flocculants, such as polyacrylamide and chitosan connect the dispersed particles, creating larger forms – flocks (Badawi et al. 2023). The following process can be seen in Figure 1. The flocculation takes use of the desolubilization of the polymer, which functions as a net to entrap the emulsions. This is crucial in case of oil-water emulsion flocculation mechanisms (Lamanna et al. 2023).

2.5.1 Coagulants

Iron Sulfate (PIX 113)

Iron Sulfate is an inorganic coagulant based on trivalent ion Fe^{3+}. It is said to be an excellent coagulating agent in water treatment and sewage treatment processes. PIX 113 is also tested in various research studies as an oil coagulant. It is said to be one of the most beneficial methods of sludge conditioning, bringing up destabilization and flocculation to the solutions (Kamizela, Worwąg, and Kowalczyk 2023).

$CaCl_2$

$CaCl_2$ is substance used in coagulation and flocculation processes, that is easily available and has a better environmental impact than metal salts, which are often used in those processes. $CaCl_2$ is rather used as a co-coagulant in coagulation and flocculation studies. According to research done by (Hägg 2015), none of the tested doses of $CaCl_2$ can replace completely primary coagulant of the reaction. Nevertheless, when the dose of the primary coagulant was reduced, it benefited from small additions of $CaCl_2$. This can be explained by analyzing the Ca^{2+} which carry the ability to reduce the repulsive forces between the particles in suspension and support charge neutralization (Hägg 2015). $CaCl_2$ has the potential to reduce usage of primary coagulants, which means that less undesirable contaminants (such as manganese) will be introduced to the environment (Gonzalez-Perez, Hägg, and Duteil 2021).

2.5.2 Synthetic Flocculants

Cationic Polyacrylamide (Praestol 851 TR)

Praestol 851 TR is a polymer (polyacrylamide) with high molecular weight, which carries a positive charge and is attracted to negatively charged particles. That water-soluble substance are created by copolymerization of acrylamide, carrying multiple positively charged monomers. This flocculant can be present in two forms – liquid or dry solids. The suggested concentration range is within 0,1 to 0,5 percent. Praestol has various applications among wastewater treatment, it can be a part of clarification, filtration and sludge dewatering processes as well as it is applied in enhanced oil recovery processes. (Anon n.d.-i).

2.5.3 Bio Flocculants

Cationic Starch - cationic 2-hydroxy-3-(trimethylammonium) propyl starch)

Over the years, flocculants based on starch have been utilized in the treatment of water, since they are inexpensive, environmentally friendly and effective when used in small amounts. Due to its structure, starch can be simply modified by adding various functional groups to its hydroxyl groups present in the saccharide ring, which enables easy modification to meet a wide range of implementations. According to previously done studies, starch is a positively charged coagulant used for negatively charged emulsions in order to neutralize them. Starch is often compared to chitosan when it comes to environmentally friendly coagulants and it is significantly more affordable natural resource (Kocaman and Yildiz 2023).

Chitosan

Chitosan (N-acetyl-d-glucosamine) is said to be one of the most promising alternatives for enviromental friendly coagulants. It is known for its biocompatibility, biodegradability, adsorption capacity as well as flocculation ability, which is the most valuable trait. As a byproduct of the fish food chain, it is a polyelectrolyte polysaccharide, that is extracted

from chitin, which is an element that with proteins creates an exoskeleton for crustaceans. This polymer is sensitive to pH changes. It will dissolve within acidic environment, and desolubilize / flocculate when the pH is changed back to basic. According to previously done studies, chitosan is a coagulant used for negatively charged emulsions (Wang et al. 2012).

Aragose

Aragose is a natural product, that is obtained from seaweed. It is an anionic polysaccharide, which carries hydrogel properties. Depending on the concentration and temperature, it can transform from a colloidal solution into a gel structure (Poologasundarampillai and Nommeots-Nomm 2017).

Extracellular polymeric substances (EPS)

Microbial extracellular polymeric substances (EPS) became a promising alternative to currently used specifics such as polyacrylamides, polyethylene oxide and polyethyleneimine. (Ajao et al. 2021). EPS can be created by pure or mixed cultures, which can be taken from microbial biochemical secretions. It can be either produced as a single type of EPS or using a mixed culture approach. The standard method of producing a single type of EPS, in the form of polysaccharides, is to enrich the pure cultures with single organic substrates (glucose). Although this strategy gives biodegradable EPS, the method itself needs sterile conditions and expensive carbon sources which are limiting factors of the process. The mixed culture approach is more convenient in the case of production conditions and feedstock. To produce EPS with this approach, low-cost feedstock, in the form of organic wastewater, can be used. What is more, the process do not require sterility conditions. As a result of the mixed culture method, a heterogeneous and heterodispersed EPS matrix is being produced, which includes different compounds with different molecular weights (MWs) and charge densities (CDs). Those are necessary parameters, particularly MW which is crucial for the flocculation process (Ajao et al. 2021).

The structure of EPS is complex since it consists of different functional groups, which respond differently to environmental factors. One of the crucial parameters for EPS performance is pH. The deprotonated and protonated states can differ between functional groups and can vary greatly depending on the pH. It can have a substantial impact on the flow behavior, organic adsorption, metal binding capabilities and the flocculation ability of EPS. According to study (Wang et al. 2012), functional groups such as carboxyl (-COOH) and amino (-NH2), present in EPS obtain more dense and compressed structures given a lower pH, due to the hydrophobicity and intermolecular hydrogen connections. The measurements done in the following research show that the pH point, where a molecule is electrically neutral (isoelectric point) is near pH 4,8 and the highest flocculation efficiency can be obtained there (Wang et al. 2012).

3. Materials and Methods

3.1 Sample's origin and preparation

The oily water tested throughout this research was a mixture of pyrolysis oil with water. For the oil water solution, 1% of oil was used in the solution, 10ml of oil was added to 1l bottle. The solution was placed on a stirrer and mixed constantly to keep the emulsion homogenous.

The **EPS I** and **EPS II** were extracted in different locations in Europe, having different element content as well as different amounts of carbohydrates and proteins in their structure. EPS is the Kaumera, which is a bio-based resource that was collected from wastewater treatment plant. EPS I was collected in Utrecht WWTP in the Netherlands, whereas EPS II was collected in Faro WWTP in Portugal.

The properties of EPS I and EPS II were calculated based on the sample measurements. Dry EPS I and EPS II samples were taken and treated with 105 C and 550 C in order to get the dry matter, ash content and volatile solids. The carbohydrate content and protein content was given by the EPS provider. The results are presented in Table 1.

Table 1 – Properties such as dry matter (DM), ash, Volatile Solids (VS), carbohydrate content and protein content all represented in [%] for EPS I and EPS II.

	DM [%]	ASH [%]	VS [%]	Carbohydrate content [%]	Protein Content [%]
EPS I	96,34	12,89	83,45	14,81	27,88
EPS II	69,93	13,61	56,32	9,5	39,74

To prepare EPS solutions for the tests, 4g of EPS was supplemented with 8g of dowex, to make sure the EPS essence is as active as possible and no calcium is present in the solution. The solutions were diluted in 100ml of distilled water. After adding all of the additives, the solutions were mixed and the pH was adjusted to pH10, since both dowex and EPS will make the solution more acidic. To adjust it, one droplet of NaOH (25%) solution was used. The mixing should remain until all of the EPS is dissolved in distilled water. The next step is to adjust the pH to 7, using HCl solution. Having that the prepared EPS solution should be left in the fridge overnight and can be used the next day.

Figure 3 – The picture on the left-hand side shows the preparation of the EPS solutions, on the right EPS II structure from the closeup can be seen

The last two EPS II solutions made had a higher concentration of EPS, instead of 4g, 8,59g was used. It was increased in order to get similar carbohydrate content between EPS I and EPS II.

3.2 Coagulants/flocculants and additivies

For the coagulation/flocculation tests, the following substances were tested: Kem Sep (FP – 101), Praestol 851 TV, Iron Sulfate (PIX 113), St Floc (Starch), Calcium Chloride ($CaCl_2$), EPS I and EPS II.

St Floc (starch) 0,2% solution was prepared using 0,2g of powder, dissolved with 100ml of distilled water. The solution was mixed until the powder dissolved fully.

Kem Sep 0,2% solution was prepared using 0,2g of powder, dissolved with 100ml of distilled water. Then, 200µL of acetic acid (CH_3COOH) was added. The solution was mixed until the powder dissolved fully.

Praestol 851TV was prepared in the same way as St Floc flocculant, 0.2g of powder in 100ml of distilled water, but it turned out that 0,2% concentration of the solution was too high and the overdosing of the coagulant could be seen. The 0,2% solution needed to be diluted again to get 0,02% concentration, which was used throughout the further research.

Iron Sulfate (PIX113) was prepared from the liquid form, where 11,7g of the solution was added to 100ml of distilled water (1:10). The solution turned out to be too acidic, so the coagulant was diluted in proportions 1:100 and used throughout the further research.

Chitosan - Kitoflokk 0,2% solution was prepared in the same way as Kem Sep, using 0,2g of powder, dissolved in 100ml of distilled water. Then, 200µL of acetic acid (CH_3COOH) was added. The solution was mixed until the powder dissolved fully.

Calcium Chloride ($CaCL_2$) solution was prepared using 3,08g of the substance with 100 ml of distilled water. The amount of charge for $CaCl_2$ should be equivalent to the charge of Kemira Pix 1:10.

Superfloc 1% was prepared by adding 1 ml liquid solution into 100 ml of distilled water. The solution was mixed until the total dissolution.

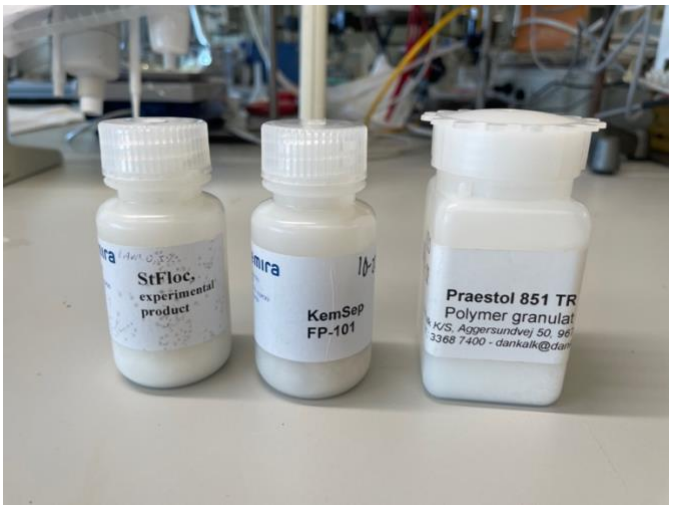

Figure 4 – Picture of coagulants used in the research – St Floc (starch), KemSep and Praestol 851 TV

3.3 Instruments and Methods

Turbidity was used as a measure of clearance of oil water after the flocculation process. A portable turbidity meter - Turbimax CUE25 – was used. The device uses light scattering techniques, within a range of 0 – 1100 NTU.

Centrifugal force was applied to encourage the separation of emulsions and to guarantee that samples are out of the water phase. The Centrifuge Sigma 3-16L was used in case of the samples, which needed more clarification and separation, before further measurements. The applied force for all of the measured samples was 3000 m/s^2 for 5 minutes.

BTEX is a group of organic compounds, that include benzene, toluene, ethyl benzene and xylenes. Those compounds are harmful and concerning when introduced to the environment. Testing for BTEX is useful when it comes to measuring the level of contamination of the previously mentioned compounds (Ahmad Allahabady 2022). In this research, BTEX measurements were used as a supplement to the turbidity measurements of the samples. BTEX measurements were done on Varian Cary 50 Bio UV-Vis Spectrophotometer, on a wavelength 260nm. The samples for BTEX measurement were diluted in propylene – 0,05ml of the sample with 4,95ml of propylene. Although

hexane is typically used for BTEX measurements, this research utilized propanol for safety reasons. Propanol also offers an acceptable correlation between absorbance and concentration.

Zeta potentials, particle size and viscosity

The Zeta potentials were measured for EPS I and EPS II. For each EPS, different pH values were tested – 2, 4.5, 6, 7, 10 to get the full picture of the zeta potential. To fit into the measurement range, each distinguished pH sample was diluted significantly - 1:10000 times with distilled water. For all of the zeta potential measurements, The Malvern Nano Zs Zetasizer was used. The same machine and sample preparation was used to measure the particle size diameter [nm].

The viscosity measurements were proceeded for EPS I and EPS II. The viscosity [cP] was tested across different pH values – 2, 4.5, 6, 7, 10 - to get the full picture of its behavior in EPS I and EPS II. Viscosity measurements were done on the portable viscometer, Viscolite 700.

Fourier Transform Infrared Spectroscopy measurements

The Fourier Transform Infrared Spectroscopy (FTIR) uses infrared light at various wavelengths in order to measure the adsorption and emission spectra. In chemistry, it is used to identify organic and inorganic materials. When the FTIR measurement is done, one can distinguish different functional groups present in the sample structure (Anon n.d.-f). For FTIR measurements in this research, EPS I And EPS II samples were used. They were previously grained into powder form and tested on the FTIR spectrometer.

3.4 Coagulation experiments

For the experiments with different coagulants, the same procedure was used throughout the research. 10 sample tubes were filled with 5ml of oil-water, which was uptaken while being constantly mixed, to make sure the emulsion was homogenous. Then the different doses of coagulant were applied.

Figure 5 – 10 sample tubes filled with oil water and coagulant – EPS I + iron sulfate (pix113)

For EPS I, EPS II Calcium Chloride or Iron Sulfate (Kemira Pix 113) was used as a co-coagulant in the reaction. For the superfloc coagulant, which is anionic, iron sulfate was used as well, to neutralize the charge and indicate the reaction. When it comes to the EPS I, EPS II dosages in the examined samples, 500μL was added to each of them. The dose of Calcium Chloride and Iron Sulfate was changed throughout each measurement. Depending on the coagulant, different doses were applied to test the efficiency of the reagent, they were usually within a range 50μL - 5000μL.

For all of the tested coagulants, the turbidity was measured. The BTEX measurement was done on some of the samples to complement the BTEX results.

4. Results

4.1 Fourier Transform Infrared Spectroscopy (FTIR) of EPS I and EPS II

The FTIR analyses was performed to identify specific functional groups of EPS I and EPS II to compare the chemical properties between the two of them. EPS samples used in this experiment were taken from two distant locations, so seeing the similarities and differences in their chemical structure is valuable. Comparing them can show whether their origin can affect their structure and can reveal differences in their composition.

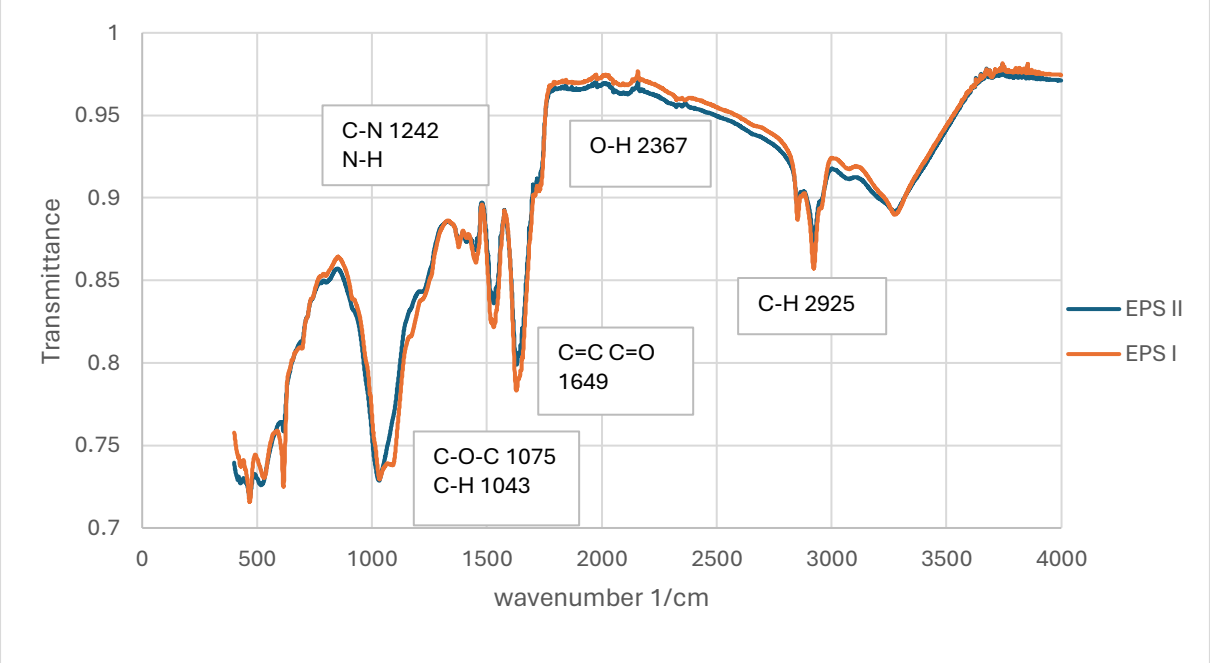

Figure 6 – FTIR spectra of EPS I and EPS II

Some of the characteristic functional groups were found on FTIR spectra on Figure 6. Starting from the left side of the graph, peaks at 1075 and 1043 correspond to polysaccharides and nucleic acids. EPS I, which is marked in orange, shows better recognition of those two peaks, whereas EPS II shows it as one. At 1242 peaks corresponding to nitrogen and amine groups could be seen. There is no significant difference between those jumps when looking at compared samples. At 1649, two groups C=C and C=O can be seen. Those are recognized as proteins. In this case EPS I shows a bit deeper peak than EPS II, but again minor differences can be seen between those two. Peaks at 2367 represent O-H which might correspond to acid groups present in the samples. At this wavenumber, it can be observed that EPS I has slightly bigger transmittance values than EPS II. An intensive peak at 2925 belongs to alkane group, again for both samples it seems to align.

4.2 pH impact on EPS I and EPS II

Zeta Potential and Viscosity

On 24.05 the zeta potential measurements were done within EPS I and EPS II samples, with different pH variations – 2, 4.5, 6, 7, 10. Viscosity was measured on the same day, in relation to changing pH. Both data are represented on Figure 7.

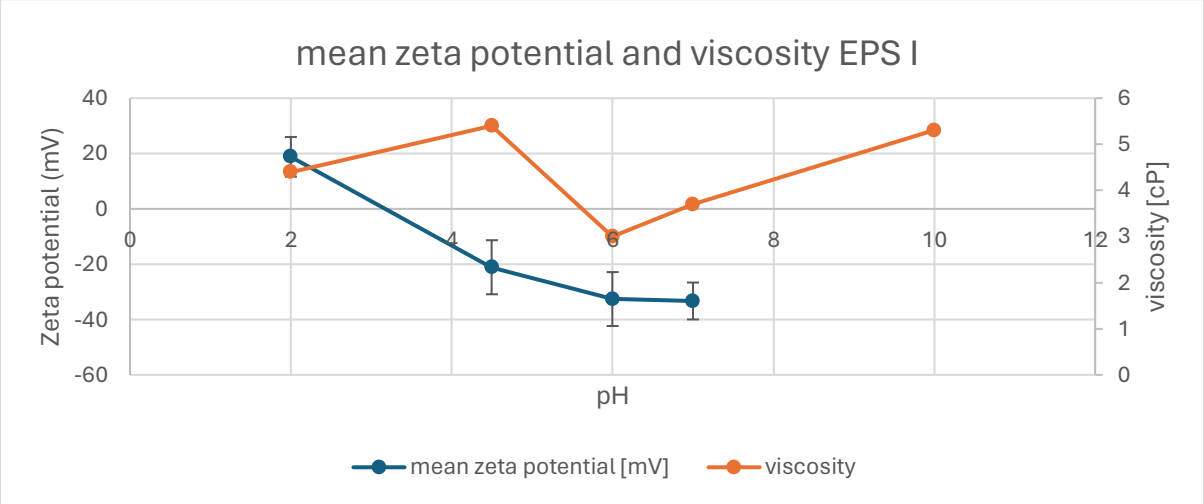

Figure 7 Viscosity measurements for EPS I compared with zeta potential measurements, throughout different pH values

The zeta potential measurement for was also done for pH10, however, due to the troubles with measuring there and odd results, that point was excluded from the plot. At pH 2 both, zeta potential and viscosity are relatively high. With increased pH to 4.5, the zeta potential decreases and viscosity is following the same trend dropping rapidly. At pH 6, the zeta potential reached most negative value around -30 [mV] . At this point viscosity reaches its lowest point as well. With increasing pH, the zeta potential remains stable and the viscosity starts to rise again.

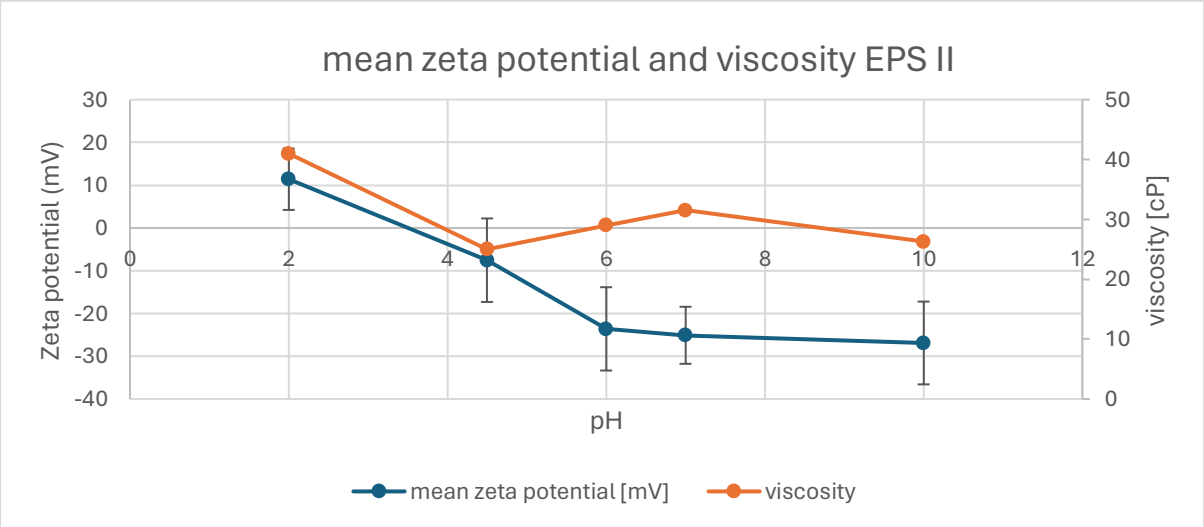

Figure 8 - Viscosity measurements for EPS II compared with zeta potential measurements, throughout different pH values

Figure 8 displays the relationship between mean zeta potential and viscosity measured for EPS II for different pH values. Both functions show a trend and clear relationship with one another. At pH2, zeta potential and viscosity are relatively high. With pH increase to 4.5, both zeta potential and viscosity, decrease, where zeta potential reaches value close to zero. At pH 6, the zeta potential still remains within the negative trend, whereas the viscosity rises and remains relatively constant. At pH10, zeta potential remains negative, while viscosity starts to decrease.

Zeta potential and size

On 24.05 the size measurements were done within EPS I and EPS II samples, with different pH variations – 2, 4.5, 6, 7, 10. Figure 24 displays the relationship between zeta potential and viscosity, measured for EPS I.

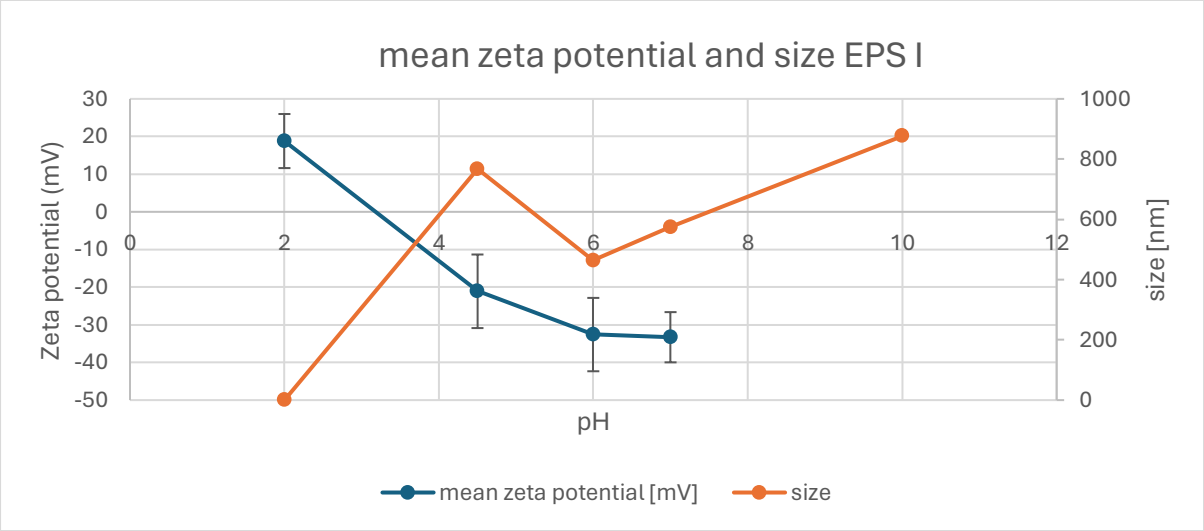

Figure 9 – Size [nm] measurements for EPS I compared with zeta potential measurements, throughout different pH values

The zeta potential measurement represented in Figure 9 was also done for pH10, however, due to the troubles with measuring there and odd results, that point was excluded from the plot. At pH 2, the zeta potential is above zero, having the highest positive value at 20 [mV]. At the same pH, the size reached the lowest value throughout the whole measurement which is around 0 [nm]. From pH 4.5 to 7, the zeta potential remains within negative trend, stabilizing around -30 [mV]. Whereas, the particle size increases rapidly at pH4,5, and decreases at pH 6, where zeta potential remains negative and stable. At pH 10, an increases in size can be seen again, reaching it's highest value of 800 [nm].

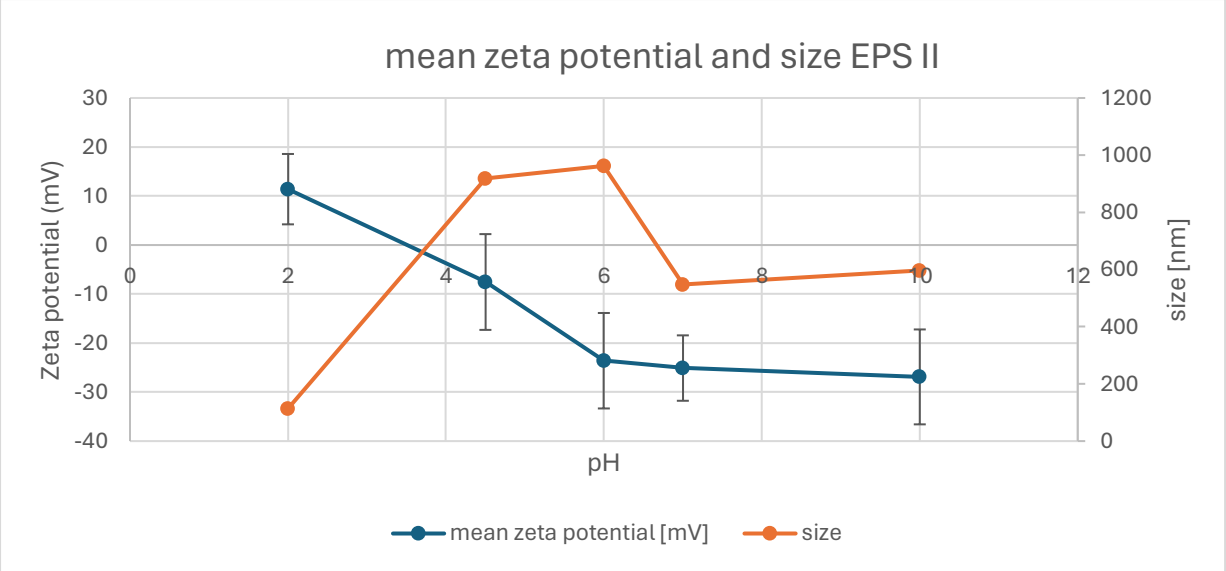

Figure 10 – Size [nm] measurements for EPS II compared with zeta potential measurements, throughout different pH values

Zeta potential and size measurements for EPS I are displayed in Figure 10. At pH 2, the zeta potential is above zero, having the highest positive value at 10 [mV]. At the same pH, the size reached the lowest value throughout the whole measurement which is around 100 [nm]. The change in pH occurs between pH 2 and pH 4.5, that's where the isoelectric point is located. From pH 4.5 to 6, the zeta potential remains within negative trend, stabilizing around -25 [mV]. Within pH 6 to 10, the zeta potential remains stable oscillating around -25 [mV]. The particle size increases rapidly at pH4.5, and stabilizes at pH6, where zeta potential remains negative and slowly stabilizes. At pH7 there is a stabilization in zeta potential, whereas the size rapidly drops. At pH10, the size and the zeta potential stabilize.

BTEX EPS II

Figure 11 represents the BTEX measurements of EPS II in oil-water measured within pH range from 2,4 to 7,6.

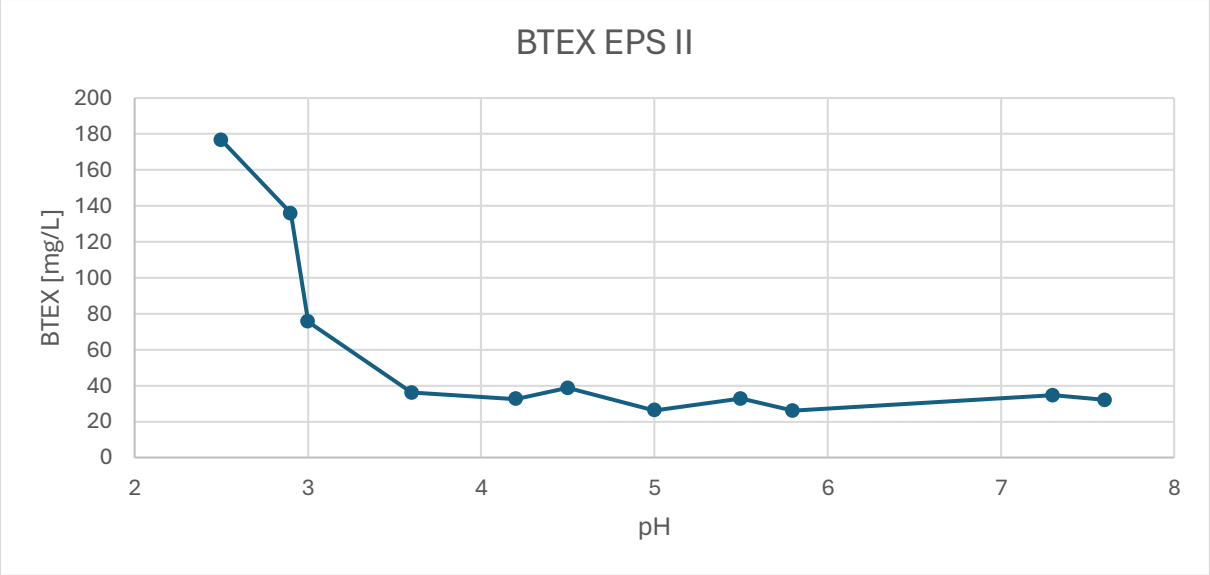

Figure 11- BTEX measurements for EPS II in oil-water emulsion, measured for a pH 2,4 to 7,6

Figure 11 shows how pH variations affect the EPS II BTEX. Within acidic pH range from 2.5 to 3.5, the BTEX results were relatively high. As the pH changed into more neutral / alkaline, the values start to decrease and become more stable. Throughout the rest of the measurements within pH 4,5 to 7,5, the values remain low oscillating between 20-40 mg/L.

4.3 Testing the coagulants – Turbidity and BTEX measurements

Aragose + CaCl2

Testing Aragose and $CaCl_2$ as a coagulant was conducted twice, on 27.02 (1st trial) and on 5.03 (2nd trial). Turbidity in the samples was measured and plotted on a graph 12 for better visualization of the results. The pH of the samples before adding the coagulant was around pH 8. To make sure that all of the readings fit the turbidity meter range, the samples were diluted with distilled water (filled up to 10ml) and centrifuged 3000m/s^2 for 5 minutes.

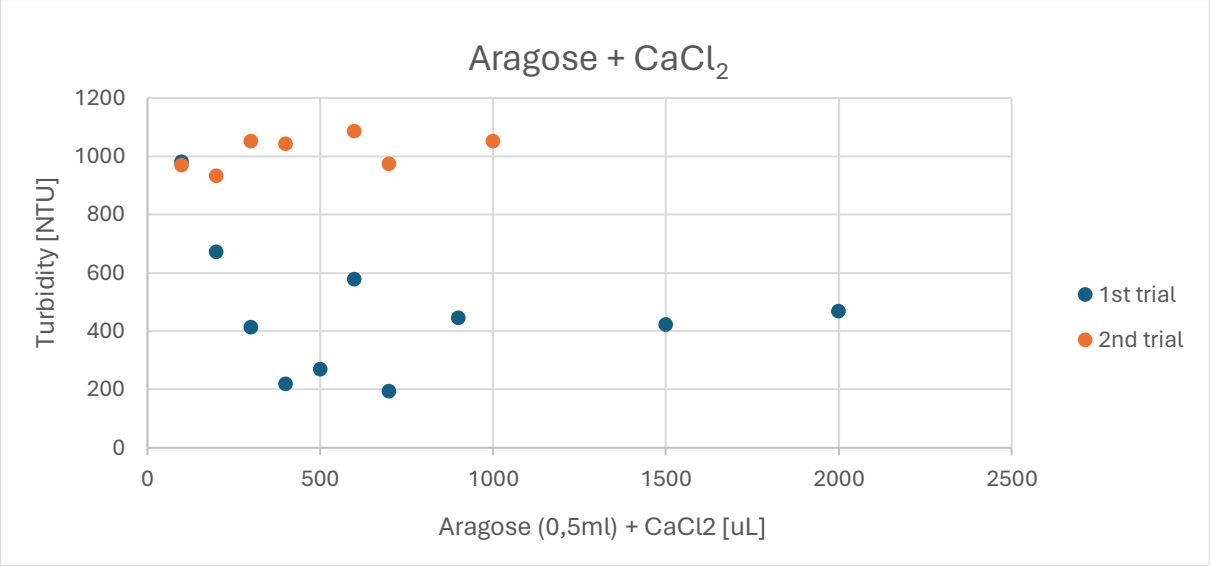

Figure 12– Turbidity measurements on samples with Aragose and $CaCl_2$ as a coagulant

The results from those two measurements do not show similar results. The first measurement (27.02) shows a promising result – 200 [NTU] within the range of 500 $CaCl_2$ dose. As the dose of $CaCl_2$ increased, the turbidity raised a bit and flatten out within turbidity range around 400 [NTU]. The second measurement (5.03) shows high turbidity results, which remain within the range of 1000 [NTU].

Figure 13– Picture of the samples from the second measurement (5.03) with Aragose and $CaCl_2$ as a coagulant

Figure 13 shows how the coagulant worked during the second measurement (5.03). The changes could be seen right after adding a coagulant to oil-water and mixing of the samples. In all of the samples the floc creation occurred. The created forms were settled not only at the top but also the smaller floc formations were dispersed around the samples. The turbidity measured and displaced on Figure 12 shows that for the second

trial, the results were high and the coagulant did not perform well, although looking at the samples on Figure 13, the changes could be observed.

Cationic Starch

Testing St Floc (starch) as a flocculant was conducted twice, on 27.02 (1st trial) and on 4.03 (2nd trial). The samples had pH around 8. St Floc was tested again on 5.04, this time with pH adjusted to 7. Turbidity in the samples was measured and plotted on a graph 14 for better visualization of the results.

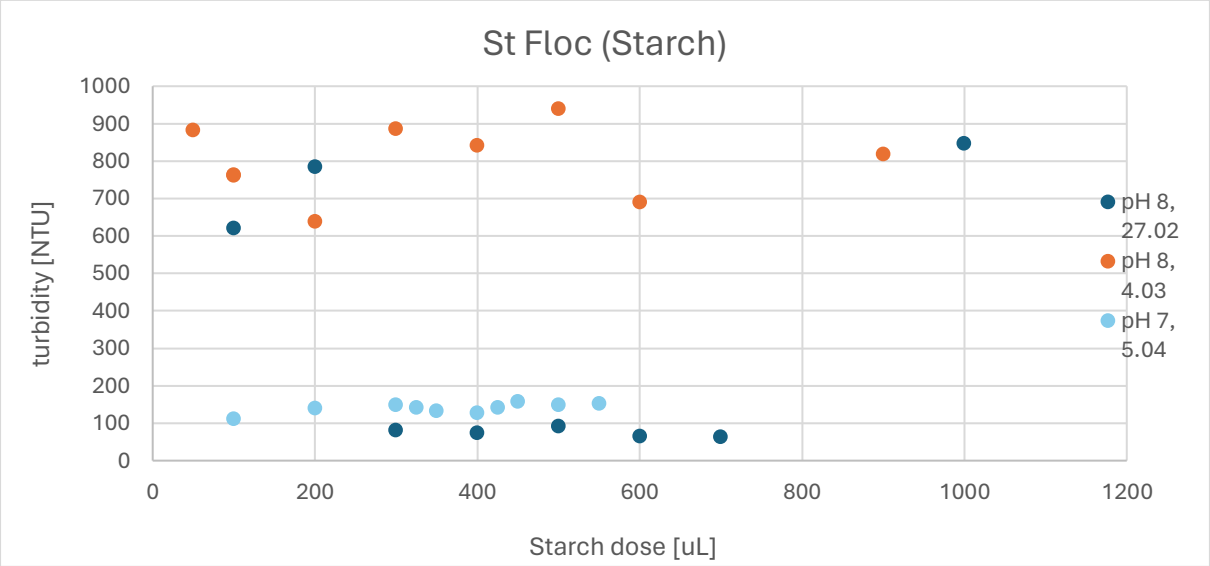

Figure 14– Turbidity measurements on samples with St Floc (Starch) as a flocculant with pH adjustment

The results carrying the same pH (8) show inconclusive results. The results from the 27.02 show that in between dose 300 and 700 [µl] the turbidity was the lowest, oscillating around 100 [NTU] which is a really promising result. The second trial (4.03) with starch as a flocculant gave high results in turbidity and did not match previous results even though the doses for both trials were matching. The samples measured on 5.04, where the pH was set to pH 7 showed the best results throughout the whole measurement. From the dose 100 to 700 [µl] the turbidity remained between 100 and 200 [NTU]. Some of the points from 1st measurement (27.02) where pH was set to 8 and from the last one (5.04), where the pH was set to 7 match and give really promising results regarding the pH change.

Cationic Polyacrylamide (Praestol 851 t)

Testing Praestol 851tr was conducted on 5.04. The pH of the samples before adding the flocculant was around pH 8. Turbidity and BTEX in the samples was measured and plotted on a graph 15 for better visualization of the results.

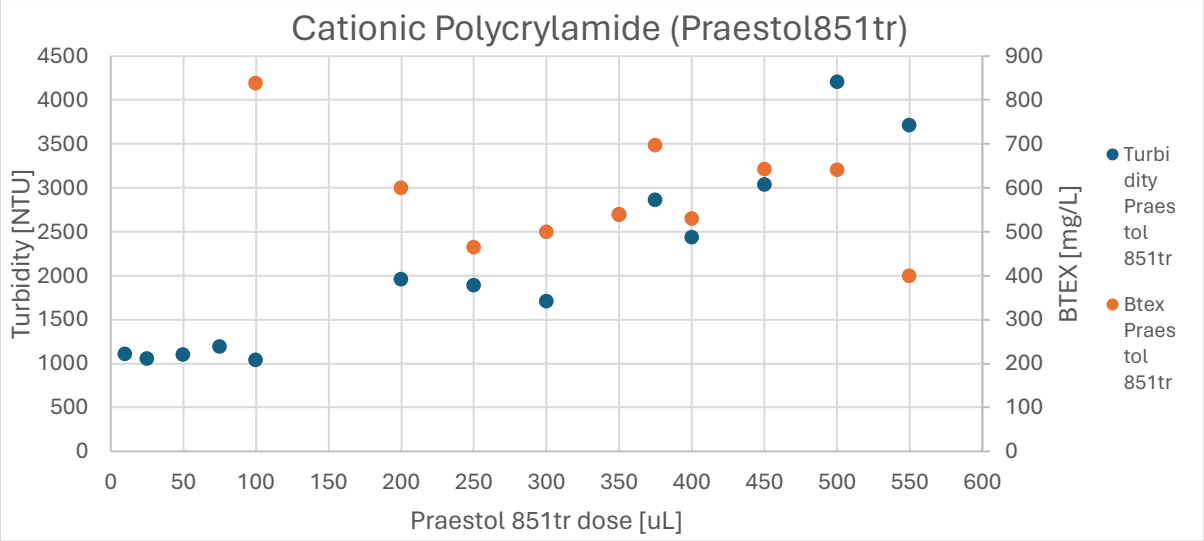

Figure 15 – Turbidity and BTEX measurements in samples with Praestol 851 TV as coagulants, with pH 8

The turbidity results for Praestol 851 Tr show results that oscillate between 100 and 400 [NTU]. The lowest turbidity was obtained within range of 10 to 100 [µl], which means that the flocculant worked most sufficient within that range. With increasing dose of flocculant, the turbidity rose. That might indicate that thee overdosing of flocculant appears. The BTEX measurements were done to complement the turbidity measurements for Praestol 851tr as a flocculant. The results obtained from the measurements oscillate between 40 to 80 mg/l. While comparing turbidity and BTEX results it is visible that they share a similar trend excluding the first measurement which was done at 100 [µl].

Figure 16– Picture of the samples with Cationic Polyacrylamide (Praestol 851tr) as a coagulant

Figure 16 shows how the flocculant worked during the different doses applied. It can be seen how throughout different flocculant doses, the oil started to separate from water

creating floc formations. In all of the doses the flocs occurred and settled in the top layer of solution.

Kem Sep

Testing KemSep was conducted on 5.04. The pH of the samples before adding the flocculant was around pH 8. Turbidity in the samples was measured and plotted on a graph 17 for better visualization of the results.

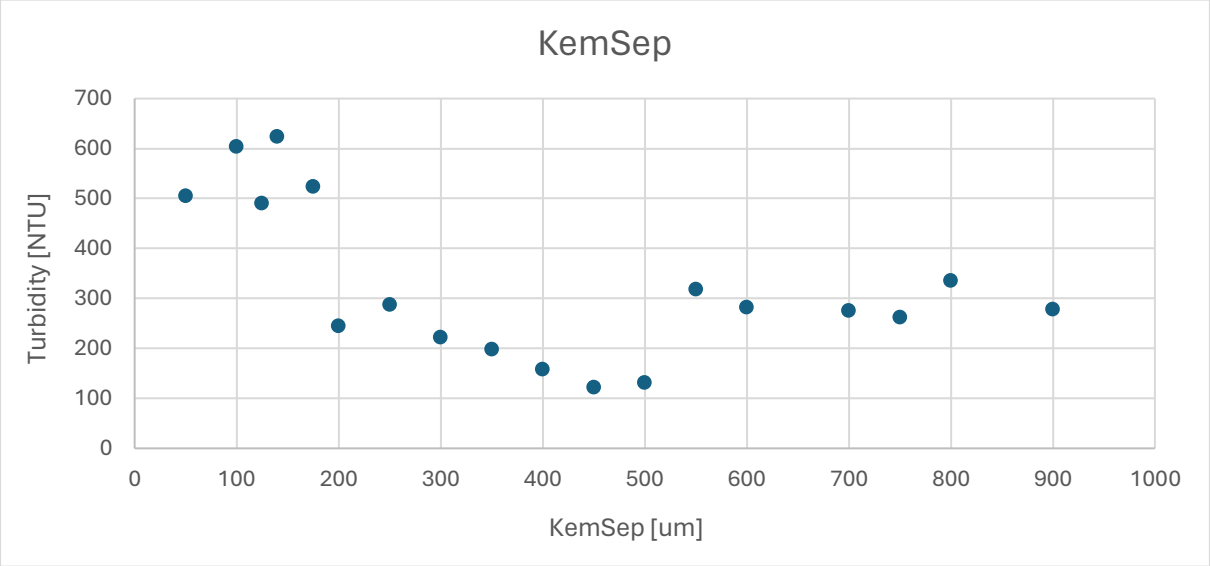

Figure 17– Turbidity measurements in samples with KemSep as a flocculant, with pH 8

The turbidity results for KemSep oscillate between 100 and 600 [NTU]. For small doses of flocculant (0 – 175 [µl]), the results show the highest turbidity 500 – 600 [NTU].

The lowest turbidity was obtained for flocculant dose 450 [µl] and within that dose range, the flocculant worked best. With an increasing dose, the turbidity remained stable with turbidity swinging back and forth around 300 [NTU].

Kitoflokk (chitosan)

Testing kitoflokk was conducted on 5.04. The pH of the samples before adding the flocculant was around pH 8. To make sure that all of the readings fit the turbidity meter range, the samples were diluted with distilled water (filled up to 10ml) and centrifuged 3000m/s^2 for 5 minutes.

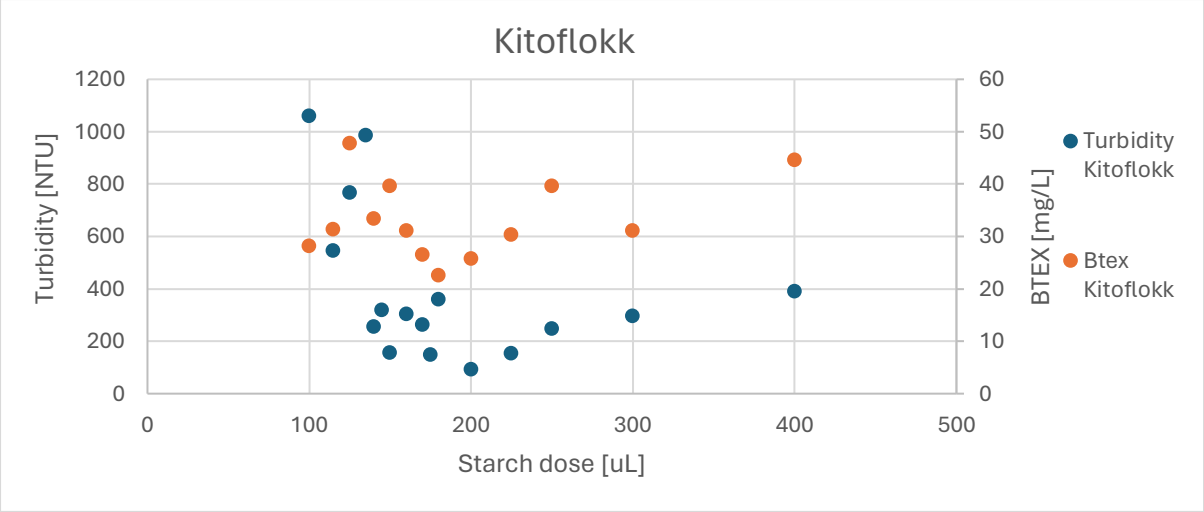

Figure 18– Turbidity and BTEX measurements in samples with Kitoflokk as a flocculant, with pH 8

The results for kitoflokk show expected turbidity results. The best flocculant performance can be seen between 120 and 220 [µl], where the turbidity oscillates between 50 and 300 [NTU]. The best turbidity result was obtained where kitoflokk concentration was 200 [µl]. After dose of 200 [µl], the turbidity started to rise, proportionally to the added dose of flocculant, achieving tubidity of 400 [NTU] at the dose of 400 [µl]. The BTEX measurements were done to complement the turbidity measurements for kitoflokk as a flocculant. The results obtained from the measurements oscillate between 25 to 50 mg/l. While comparing turbidity and BTEX results (Figure 18) it is visible that they share a similar trend, where within the 150-200 [µl] dose of flocculant the best results were obtained.

Figure 19 – Picture of the samples from Kitoflokk samples as a coagulant

Figure 19 shows how the flocculant worked during the different doses of kitoflokk as a flocculant. It can be seen how throughout different doses, the oil started to separate from water. In the sample where 125 [µl] kitoflokk dose was added, oil droplets separation occurred, the dispersion of oil can be seen throughout the sample and the oil started to accumulate at the top of the sample. In the sample where the 150 [µl] kitoflokk dose was added, the separation occurred and the created forms settled at the top of the sample.

Superflocc

Testing superflocc as a flocculant was conducted on 5.04. The pH of the samples before adding the flocculant was around pH 8. In order to make superfloc work, iron sulfate (PIX113) needs to be added, since superfloc is an anionic substance and it will not perform without the addition of positively charged ions. To make sure that all of the readings fit the turbidity meter range, the samples were diluted with distilled water (filled up to 10ml) and centrifuged at 3000m/s for 5 minutes.

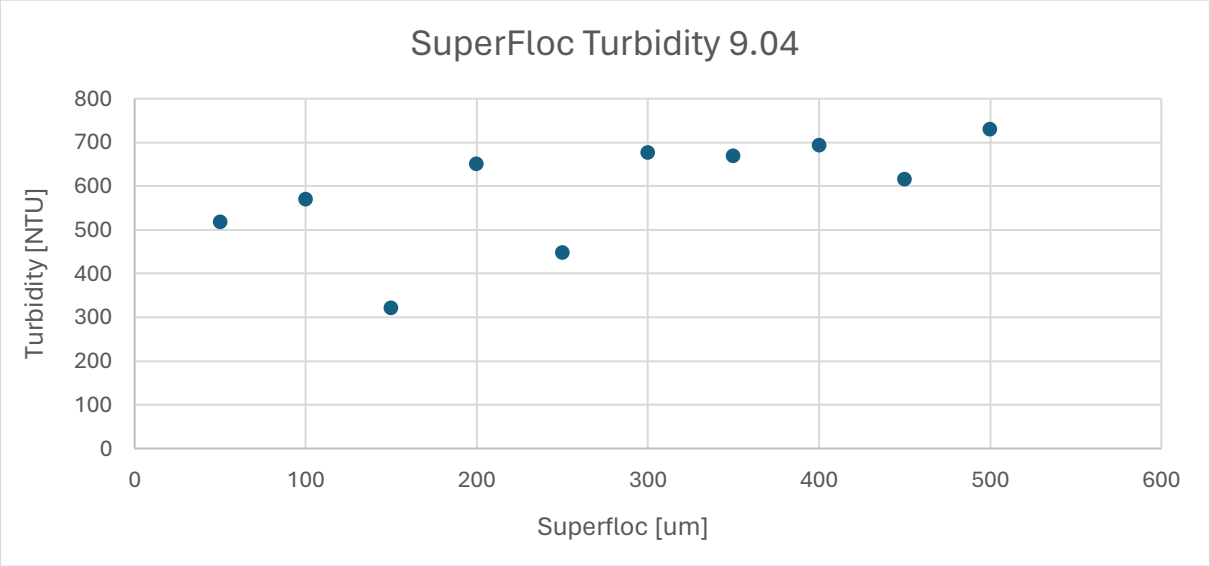

Figure 20– Turbidity measurements in samples with Superflocc and iron sulfate (pix113) as coagulants, with pH 8

The results for superfloc turbidity oscillated between 300 and 700 [NTU], which do not show any significant variation. The best turbidity result was obtained with the superfloc dose 150 [µl], giving turbidity 310 [NTU]. With higher doses of flocculant, starting with 300 [µl], the turbidity remained close to 700 [NTU], which is not promising.

Figure 21– Picture of the samples from superflocc samples as a flocculant

Figure 21 shows how the coagulant worked during the different doses of superflocc as a flocculant. It can be seen how throughout different doses, the oil started to separate from water. While looking at the sample with the dose 150 [µl] (second left) where according to Figure 20, the lowest turbidity occurred, no significant differences in the oil-water separations or clarity can be seen.

4.2 Changing the order of compounds – $CaCl_2$ + EPS I & EPS II and EPS I + iron sulfate

Testing EPS as a primary flocculant and $CaCl_2$ as a secondary coagulant was conducted a few times, with changes in the pH.

On 07.05 EPS I and EPS II with $CaCl_2$ was tested, with pH adjustment to 4. The blind measurements were done with only $CaCl_2$ as a coagulant. They were conducted for comparison purposes. Turbidity in the samples was measured and plotted on a graph 22 for better visualization of the results.

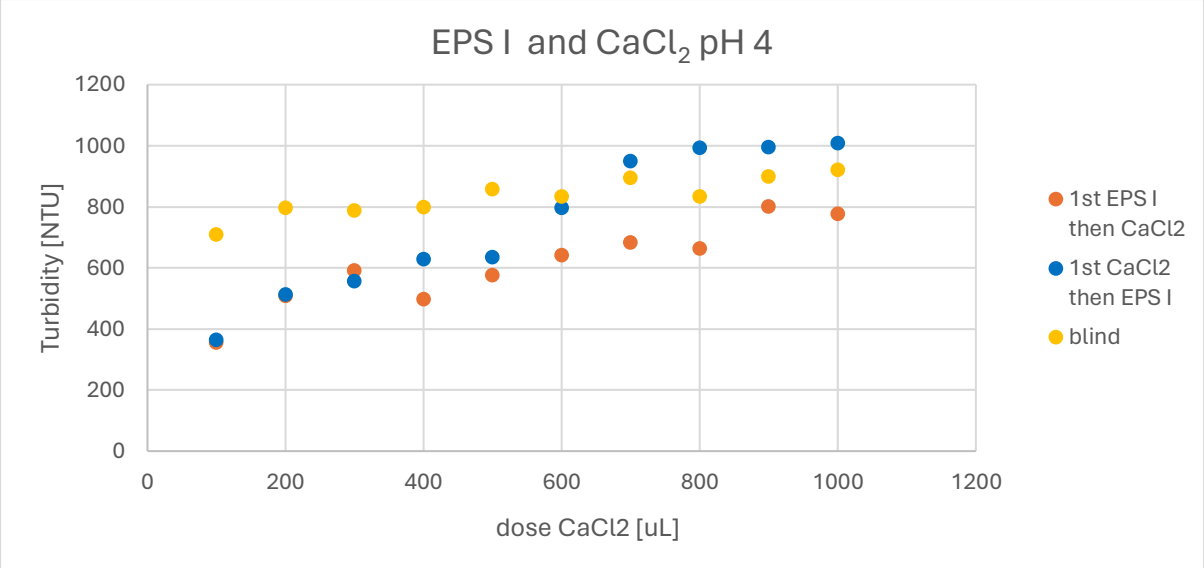

Figure 22– Turbidity measurements on samples, where the order of compounds was changed, using EPS I and $CaCl_2$ as a coagulant, with pH 4. The samples were measured on 07.05.

The results from adding EPS I as a flocculant and the samples where EPS I is added secondly show similar trend. The turbidity in the measurements rises while adding higher doses of $CaCl_2$. In the samples where $CaCl_2$ was added first, the turbidity rose above the blind sample measurements, which is odd and shows that maybe overdosing of one of the $CaCl_2$ coagulants appeared. Even though the samples where EPS I was added first showed the best results of all, they were still not sufficient and did not meet the required expectations.

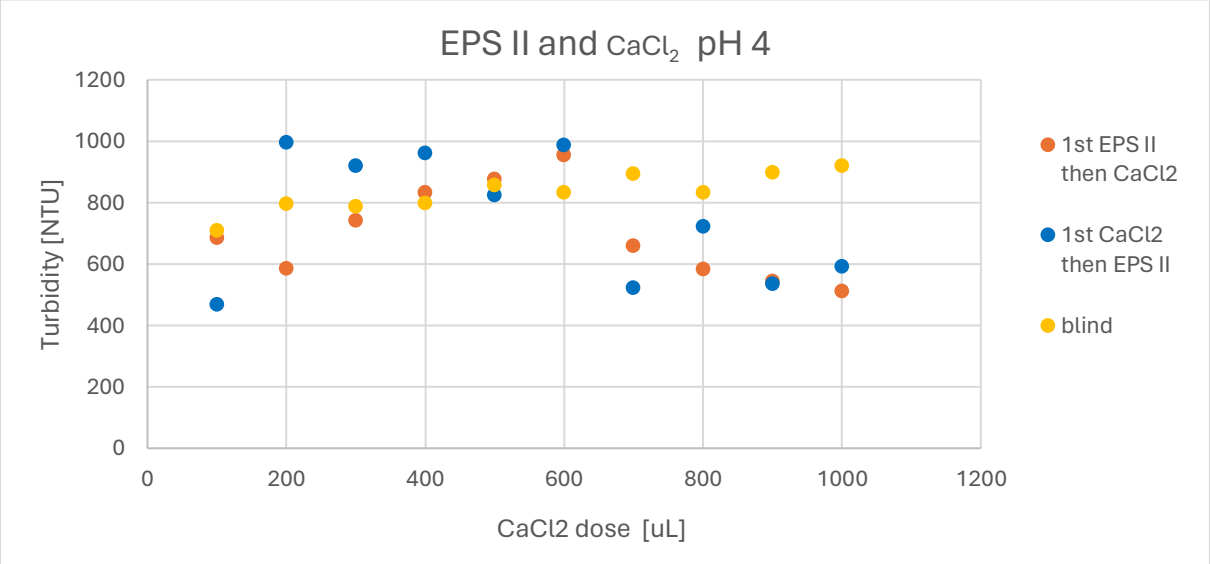

Figure 23 - Turbidity measurements on samples where the order of compounds was changed, using EPS II and $CaCl_2$ as a coagulant, with pH 4. The samples were measured on 07.05.

The results from adding EPS II as a first and then as a second substance worked best within the range 700 to 1000 $CaCl_2$ [µl]. Both, results from adding EPS II first and adding

it as a second one are similar and close to the examined blind sample. All of the results did not achieve turbidity lower than 400 [NTU].

On 17.04 EPS I and EPS II with $CaCl_2$ was tested, with pH adjustment to 8. Turbidity in the samples was measured and plotted on a graph 24 for better visualization of the results.

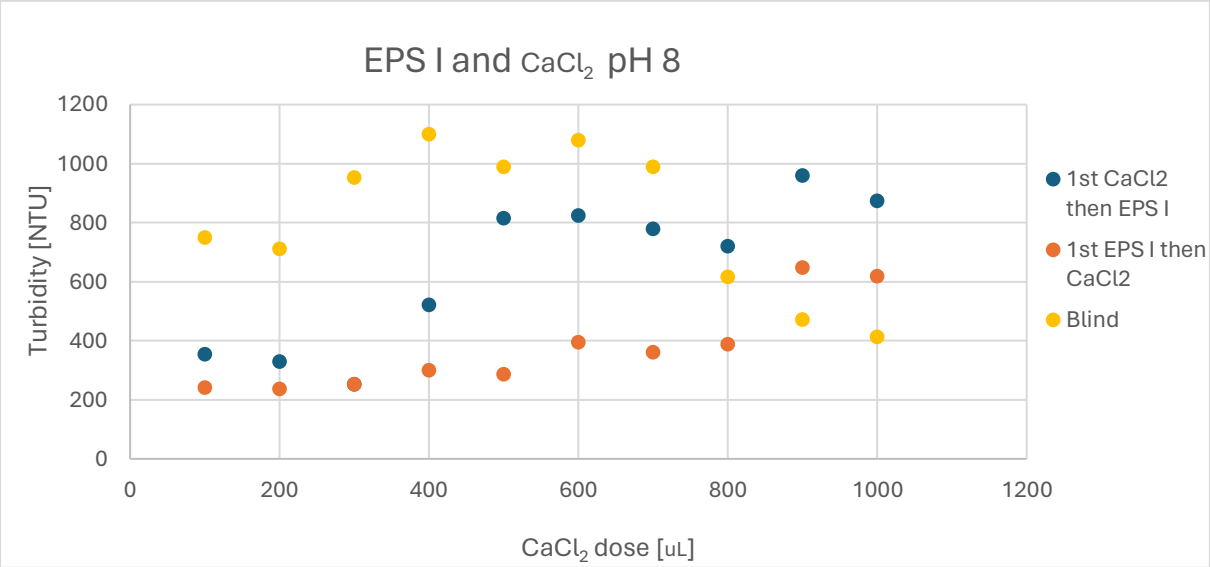

Figure 24– Turbidity measurements on samples where the order of compounds was changed, using EPS I and $CaCl_2$ as a coagulant, with pH 8. The samples were measured on 17.04.

The results from adding EPS I and $CaCl_2$ in a different order at pH 8 worked best when EPS I was added as the first one. In that case, the turbidity for most of the samples was between the range 200 and 400 [NTU], which is a promising result. The samples where $CaCl_2$ was added first worked best when small doses of $CaCl_2$ were applied (100 and 200 [µl]). For high doses (800 - 1000 [µl]) the same configuration of substances worked with no sufficient results, giving even higher turbidity results than the blind results itself. Both configurations of coagulant and flocculant worked dissatisfactory for higher doses of $CaCl_2$ coagulant.

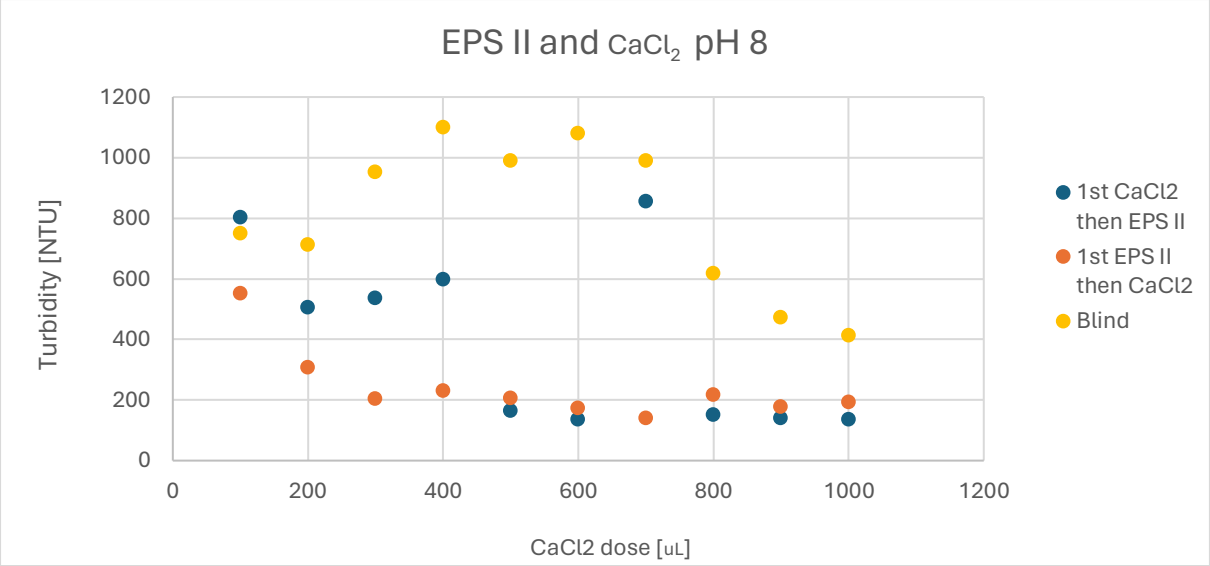

Figure 25– Turbidity measurements on samples where the order of compounds was changed, using EPS II and $CaCl_2$ as a coagulant, with pH 8. The samples were measured on 17.04.

The results from adding EPS II and $CaCl_2$ in different order at pH 8 worked promising in both cases – while adding EPS II as the first and as the second one. None of the turbidity results exceeded the blind measurement. The best results for both configurations were obtained when the dose of $CaCl_2$ was higher than 500 [µl]. They oscillated around turbidity 200 [NTU]. The samples where $CaCl_2$ was added first worked worst, obtaining higher turbidity results within lower doses.

On 07.05 EPS I with iron sulfate (PIX113) was tested, with pH adjustment to 4. The blind measurements were done with only iron sulfate as a coagulant. Turbidity in the samples was measured and plotted on graph 26 for better visualization of the results.

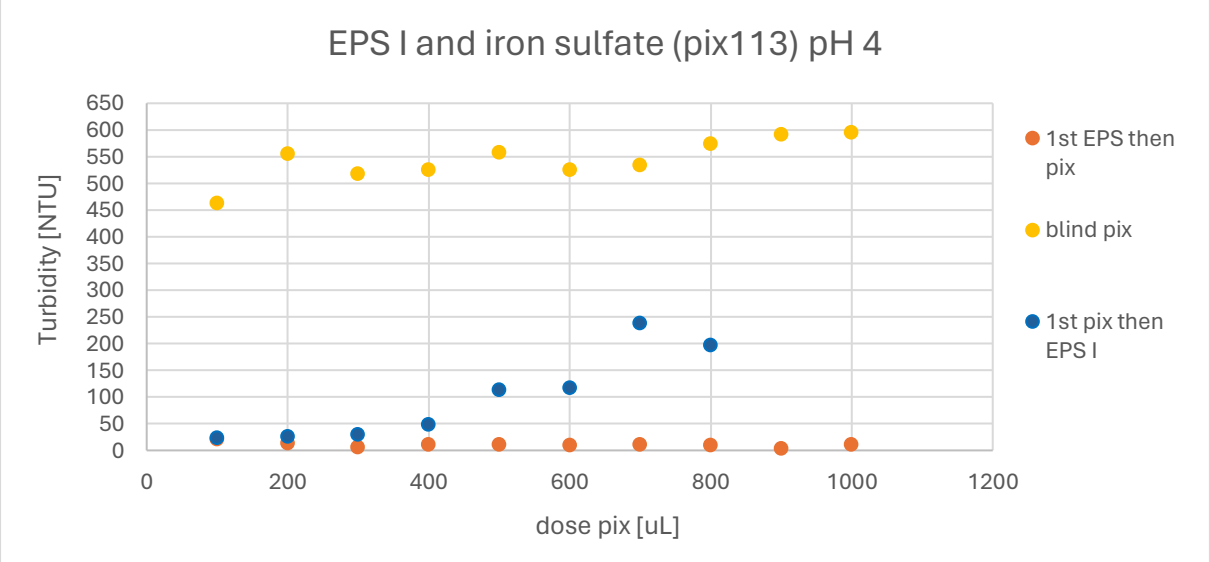

Figure 26 - Turbidity measurements on samples where the order of compounds was changed, using EPS I and iron sulfate as a coagulant, with pH 4. The samples were measured on 7.05.

The results from adding EPS I and iron sulfate to the prepared samples were successful in both configurations, the results had lower turbidity than 250 [NTU] and both were much lower than the blind iron sulfate measurement. Nevertheless, the samples where EPS I was added first, followed by the iron sulfate had great results which were oscillating close to 0 [NTU] throughout all of the doses of PIX113. The samples where iron sulfate was added first performed worse in case of higher iron sulfate doses. Starting with dose 300 μL till 800 μL, the turbidity rose and was oscillating between 100-250 [NTU].

5 Discussion

5.1 Fourier Transform Infrared Spectroscopy (FTIR) measurements for EPS I and EPS II

In conclusion to Figure 6, the similarities in presence and intensity of the peaks appearing for specific functional groups are major. Some minor changes can be seen throughout the peak intensity, which can be seen in case of protein groups, where the EPS I peak is a bit deeper than the EPS II. However, presence of all the same groups and alining of the EPS I and EPS II FTIR lines suggest that the chemical composition and structure remain the same. Fourier Transform Infrared Spectroscopy spectrum reflects similarities, showing the very same transmittance values throughout the measured wavenumber range.

5.2 pH impact on EPS I and EPS II

5.2.1 Viscosity and Zeta Potential

Referring to Figure 7, looking at the pH range 2 to 6, an opposite relationship between the zeta potential and viscosity can be seen. With decreasing zeta potential, the viscosity rises. This changes at pH 6, when, where the environment becomes more alkaline the zeta potential remains stable and the viscosity increases rapidly. Those relations between viscosity and pH show a strong correlation between one another. pH has a substantial impact on the stability of EPS I as well as on the electrostatic interactions that occur in its structure. Low viscosity can be caused by more negative zeta potentials, which may cause particle repulsion. Accordingly, zeta potential closer to zero can ease interactions between particles and enhance higher viscosity.

Zeta potential and viscosity measured for EPS II share a reverse relationship which can be seen in Figure 8. The measurements done at pH6 start to show an inverse trend within the functions, where with decreasing zeta potential, the viscosity increases. This shows how strong relation between viscosity and zeta potential (pH) occurs. When the environment becomes more neutral, going to basic (6-10pH), the zeta potential remains negative and still, without any sudden increases. Again, as in case of EPS I and measurements displayed in Figure 7, when zeta potential is close to zero, the viscosity rises, since the interactions between the particles are enhanced. With higher particle charges, more interactions between them are possible to occur. The high positive or high negative zeta potential particles drive away from each other, leading to lower viscosity.

5.2.2 Size and Zeta Potential

Figure 9 shows that there is a strong correlation between zeta potential and size within EPS I. With increasing pH, the zeta potential was gradually becoming more negative. When pH increased to 4.5, the zeta potential dropped rapidly below zero. One can

assume, that this is connected with the negatively charged groups dominating the surface charge of EPS I. It can be caused by the deprotonation of acting functional groups. From pH 4.5 to 7, the zeta potential remains within negative trend, stabilizing around -30 [mV]. At pH 2, the particle size is small, which is connected with high zeta potential (20 [mV]) in that pH point. Having a high zeta potential indicates that the optimum zero zeta potential is far, hence the interactions between particles are weak. When an increase in pH from 2 to 4.5 appears, there is a rise in particle size. The particle size within the EPS structure lies within 100nm – 1000nm which qualifies them as microparticles. The particles which are within the lower range of that scale can provide balance between surface area and bridge between the particles creating small droplets and cause aggregation. Polymers with larger particle sizes can have lower surface area relative to their volume, which means that they might end up having a small portion of their mass exposed to the surrounding environment. This can lower their ability for interactions.

The rise in particle size, might be explained by the polymer deprotonation occurring in some functional groups. Increased charges and repulsion of particles cause polymeric to elongate (Anon n.d.-a). At pH10, the size reached one of the highest values, which can be explained by deprotonation and maximum elongation of the polymers. The particle size is also linked directly to the pH. In an acidic environment, particles tend to remain small and within compact structure, which can explain really low value for size measured in pH2. Whereas when the environment changes to basic, the polymeric chains start to elongate and with their stretched-out structure, their size increases (Ofridam et al. n.d.).

The particle size is affected by the pH and zeta potential and the relationship between those two is visible in Figure 10. The particle size is low at acidic pH, rising when the pH is increased to 4.5. At this pH range, the zeta potential decreased, crossing the zero zeta potential line. This means that around that area the isoelectric point (IEP) and electric neutralization occurs. That can directly affect the size, which increases in that area. It might be explained by the polymer deprotonation occurring in some functional groups. As the zeta potential stabilizes at neutral/alkaline pH, the size remains stable, with a slight increase as well. The zeta potential in this area remains negative, keeping the system more stable. This may explain the smaller particle size within that area since no rapid electrical exchanges occur among the particles.

EPS I as well as EPS II show similar trends when it comes to the particle sizes, viscosity, zeta potentials and their relationships with pH variations. For both of them, the isoelectric point was between pH 2,4 and pH 4. Within that area, the coagulant was more active which can be seen by looking at the size measurement. Size increased within that area.

5.2.3 BTEX and EPS II

Figure 11 shows how pH-dependent is the EPS II performance. The graph illustrates that there is a clear connection between the BTEX concentration and the pH level. An acidic environment creates bad conditions for EPS II capabilities, which can be seen in high BTEX results in that area. As the pH becomes more neutral the BTEX results start to show stabilization and lower BTEX values are obtained. This can occur due to the more open structure, which provides additional sites for adsorption. That change occurs within pH 4.5, which aligns with the zeta potential measurements done for EPS II, presented in Figure 10. Within that pH range, the isoelectric point occurs, where the net charge is weakened and the particles become more likely to bind with one another.

5.3 Testing the coagulants – Turbidity and BTEX measurements

5.3.1 Aragose + CaCl2

Two test measurements for Aragose and $CaCl_2$ displayed in Figure 12, show different turbidity results for the same dose of $CaCl_2$. The two measurements do not follow each other patterns. The first trial can suggest that overdosing of $CaCl_2$ occurred, after the 700 [uL]. The second trial showed really high turbidity values across all the doses. Further investigation of whether flocculant and coagulant complement each other is needed.

From analyzing Figure 13, which is a picture from the second trial of the flocculant and coagulant together, it can be concluded that despite the high turbidity readings, the floc formation occurred. It is an expected outcome in this process. The high turbidity readings might occur due to faulty floc formation. Some of them could break apart and be resuspended in water during the measurement. There is a prove in those data that coagulation occurs, nevertheless, the data is not sufficient to state that those two substances worked well. It is easier to get one coagulant to work than to try coagulant and flocculant to cooperate in the floc formation.

5.3.2 Cationic Starch

Results displayed in Figure 14 show results for both, pH 8 and pH 7. For the trials conducted for pH 8, the measurements show inconsistent results. The trial done on 27.03 with pH 8 show promising turbidity results within the cationic starch dose range – 300 to 700 [µl]. The best results were obtained when pH was adjusted to 7. Even though the pH decrease is not that rapid, the change can be seen. Every tested dose for this trial obtained promising turbidity value. Those results obtained from testing Starch as a coagulant suggest that pH plays role in the effectiveness of the process. A lower pH value is significant to obtain the desired results. The starch as a coagulant works better within a bit acidic/neutral environment, which is aligned with the results of this experiment.

5.3.3 Praestol 851 tr

Two test measurements for turbidity and BTEX measurements checking the effectivity of cationic polyacrylamide (Praestol 851tr) are displayed in Figure 15. Looking at the results, the flocculant works best within lower doses (0 to 100 [μl]), decreasing the turbidity rapidly. The results obtained from adding higher doses resulted in overdosing, which caused higher turbidity results. This might occur due to the destabilization of already formed flocks. Another explanation might be in zeta potential which due to the overdosing is switching from negative to positive charge, creating bad conditions from creating bonds between particles. The floc formation could be seen in all of the samples, which can be seen in Figure 16. This is a promising sign since it indicates that the flocculant is effective, creating flocs. Nevertheless, with the higher doses, the flocculant becomes less effective. The BTEX measurements, used as a complementing measurement for the turbidity result, showed a similar trend throughout the experiment, excluding the first measurement done for 100 [μl].

5.3.4 Kem Sep

The results for KemSep flocculant are displayed in Figure 17. The optimal flocculant dose which was the most effective found during that experiment was equal to 450 [μl]. Adding more flocculant caused the turbidity to increase and stabilize around 300 [NTU]. This shows that adding higher doses of flocculant do not improve its performance.

5.3.5 Kitoflokk

Two test measurements for turbidity and BTEX measurements checking the effectivity of Kitoflokk are displayed in Figure 18. The best performance of the flocculant can be observed within 120 and 220 [μl] dose range, where the turbidity achieved effective reduction below 200 [NTU]. With increasing the dose of flocculant, the turbidity values rose as well. This might be caused by the overdosing of the flocculant and restabilization of the system. The BTEX measurements complementing the turbidity results showed a similar trend. The best BTEX results align with the best results obtained for the turbidity which are within the range of 150 to 200 [μl] doses of kitoflokk. The alignment of those to measurements, being most effective within the same dose, can implement that those were the best conditions for both indicators.

5.3.6 Superfloc

Results for superfloc as a flocculant were displayed in Figure 20. The lowest turbidity value 300 [NTU] was obtained for dose 150 [μl] of superfloc, which means that that's the most efficient dose in the case of this experiment. Applying higher doses do not help with efficiency of this process. Overall superfloc performance is not sufficient in case of this flocculation. This flocculant has limitations when it comes to additional coagulant which needs to be added for separation to occur. Balancing out the dosage of these two

substances might be crucial. In this case, the superfloc dose might be too high and the iron sulfate coagulant might be too low. Those changes could be made in order for this reaction to perform more efficiently.

5.3.7 Iron Sulfate (Pix113)

The addition of EPS I with addition of Iron Sulfate is effective when it comes to the separation of oil-water, resulting in almost ideal turbidity results. The measurements where EPS I was added first to the mixture gave better results than when the PIX113 acted as the first one added. The sequencing of adding the coagulant and flocculant is important in order to perform the best separation. The iron sulfate works as an effective initial coagulant, due to its high charge density. When added first to oil-water mixture it can act on the negative charges and lead to coagulation process creating first flocs. When EPS I was added, its role was to create connections between the particles between destabilized particles, which resulted in larger flocs creation.

5.4 Changing the order of compounds – $CaCl_2$ + EPS I & EPS II and EPS I + iron sulfate

Figures 22 and Figure 24 show performance of EPS I with $CaCl_2$, within different pH values – 4 and 8. The comparison of those two can show how the pH level can impact the turbidity and also, if the different order of adding compounds has an impact on the coagulation process. Figure 22 where the pH is adjusted to 4 showed increase in turbidity values with increasing the dose of coagulant, in both sequence cases. In case of adding $CaCl_2$ first, measured turbidity was higher than the blind sample measured for comparison purposes, which implies that potential overdosing has occurred. Figure 24 represents again, the sequence of the coagulant and flocculant tested, but this time within pH 8. In this case, the turbidity results remain low for samples where EPS I was added first, with promising results around 200 - 400 [NTU]. In case of the other sequence, where the $CaCl_2$ is added first, the results show higher turbidity levels, which indicate an insufficient coagulation process. This may be also caused by the fact that with the addition of $CaCl_2$, even more alkaline environment is created, causing an overreaction of the process. While comparing those two Figures and results within different pH values, for both cases, the samples where EPS I was added first succeeded with better – lower – turbidity results. The negatively charged EPS can present sites for adsorption when added to the negatively charged oil-water solution. Electrostatic and hydrophobic interaction can facilitate the oil separation. That might be the reason why the EPS I performs better when being added as a first substance. The best configuration for reducing turbidity in case of those two experiments is to add EPS I and adjust the pH system to 8. The $CaCl_2$ might need deeper optimization in case of dosage, and might be the factor that affects the stability of the system.

Figures 23 and 25 display the effects of applied flocculant EPS II and coagulant $CaCl_2$, within different pH doses (4 and 8). For samples where pH 4 was applied, the turbidity did not succeed with a value lower than 400 [NTU]. Changing the sequence of the substances do not have any significant differences in effectiveness of the turbidity. In case of flocculant addition to the environment with pH 8, the samples where $CaCl_2$ was added first had promising results within higher coagulant doses. Whereas, when the EPS II was added first, the results show optimistic values throughout most of the $CaCl_2$ doses, obtaining turbidity within a range of 200 [NTU]. To summarise the results for both pH values, the most effective turbidity measurements were obtained in the environment with pH 8. This might be due to the fact that the neutral/basic conditions suit better with those coagulant/flocculant combinations. When it comes to comparing the order of compounds, based on Figure 25, the more likely-looking values are obtained in case of adding EPS II as a first in the reaction.

While comparing iron sulfate (PIX113) and $CaCl_2$ performance as coagulants its clearly visible that even though the charges of both substances match, the performance of $CaCl_2$ still needs improvement. Iron sulfate (PIX113) is a synthetic coagulant that needs to be exchanged with natural replacement, which is why the tests for natural coagulants are implemented.

6. Conclusion

While comparing the coagulants and flocculants tested throughout this research, several showed promising results. As for the synthetic coagulants, the iron sulfate (PIX113) shows the best results when it comes to oil-water separation. When it comes to natural coagulants, the best results were obtained by cationic starch in the neutral/basic pH environment. The EPS II performance had also promising results, which qualify him as a good synthetic flocculant substitute.

When it comes to different orders of adding the coagulants/flocculants, the best performance was observed for EPS II pH 8, where when EPS II was added as the first coagulant, the system obtained promising results throughout most of the $CaCl_2$ doses. However, when the $CaCl_2$ was applied first, the obtained turbidity values showed even slightly better results but only within the 450 – 1000 [uL] dose range. Further studies and experiments on those substances could bring more specific and promising results when it comes to substituting synthetic coagulants from daily usage. It is crucial to remember that the effectiveness of the coagulants is strongly dependent on the dosage, pH and the sequencing of substances.

The effectiveness of EPS I and EPS II as a natural flocculant is highly dependent on the pH, which affects the viscosity, particle size and zeta potential of the substances. The results obtained for EPS I and EPS II accompanied by $CaCl_2$, show that they demonstrate best performance in neutral to basic environment. That aligns with the EPS II performance, which obtained the best turbidity removal efficiency at pH 8. Particle interactions and aggregations of the molecules are influenced by the isoelectric point, which is crucial to find in order to discover the best pH range for the substance's performance.

Adding iron sulfate (PIX113) as a coagulant is effective when it comes to the oil-water separation, resulting in almost ideal turbidity results. $CaCl_2$ was tested to be a substitute substance for PIX113, even though the charges of both substances match, the performance of $CaCl_2$ still needs improvement.

EPS I and EPS II are substances, which come from a different origin, carrying similar but non-identical properties (different protein and carbohydrate content). However, when it comes to analyzing the FTIR results, presence of all the same groups and alining of the EPS I and EPS II lines could be seen. It suggests that the chemical composition and structure remain the same. It implies that both, EPS I and EPS II regarding the different origination can be used for the same purposes with similar outcomes.

References

Ahmad Allahabady, Zabihollah Yousefi. 2022. “Measurement of BTEX (Benzene, Toluene, Ethylbenzane and Xylene).” 23–31.

Ajao, Victor, Remco Fokkink, Frans Leermakers, Harry Bruning, Huub Rijnaarts, and Hardy Temmink. 2021. “Bioflocculants from Wastewater: Insights into Adsorption Affinity, Flocculation Mechanisms and Mixed Particle Flocculation Based on Biopolymer Size-Fractionation.” *Journal of Colloid and Interface Science* 581:533–44. doi: 10.1016/j.jcis.2020.07.146.

Alazaiza, Motasem Y. D., Ahmed Albahnasawi, Gomaa A. M. Ali, Mohammed J. K. Bashir, Dia Eddin Nassani, Tahra Al Maskari, Salem S. Abu Amr, and Mohammed Shadi S. Abujazar. 2022. “Application of Natural Coagulants for Pharmaceutical Removal from Water and Wastewater: A Review.” *Water (Switzerland)* 14(2). doi: 10.3390/W14020140.

Anon. 2007. “Environmental, Health, and Safety Guidelines ONSHORE OIL AND GAS DEVELOPMENT Environmental, Health, and Safety Guidelines for Onshore Oil and Gas Development.”

Anon. n.d.-a. “(A) An Example of Deprotonation (at High PH) and Protonation (at Low... | Download Scientific Diagram.” Retrieved May 29, 2024 (https://www.researchgate.net/figure/A-An-example-of-deprotonation-at-high-pH-and-protonation-at-low-pH-of-an-amphoteric_fig1_360153832).

Anon. n.d.-b. “Brownian Motion - ATA Scientific.” Retrieved May 20, 2024 (https://www.atascientific.com.au/brownian-motion/).

Anon. n.d.-c. “Colloidal Solution: Zeta Potential and Electrical Double Layer | LinkedIn.” Retrieved May 20, 2024 (https://www.linkedin.com/pulse/colloidal-solution-zeta-potential-electrical-double-layer-mukherjee/).

Anon. n.d.-d. “DLVO | Practical Surfactants Science | Prof Steven Abbott.” Retrieved May 13, 2024 (https://www.stevenabbott.co.uk/practical-surfactants/dlvo.php).

Anon. n.d.-e. “Emulsion Stability Basics | Processing Magazine.” Retrieved May 20, 2024 (https://www.processingmagazine.com/mixing-blending-size-reduction/article/15586907/emulsion-stability-basics).

Anon. n.d.-f. “FTIR Analysis Beginner’s Guide: Interpreting Results | Innovatech.” Retrieved May 21, 2024 (https://www.innovatechlabs.com/newsroom/1882/interpreting-analyzing-ftir-results/).

Anon. n.d.-g. “IOP Conference Series: Earth and Environmental Science Performance and Characteristics of Bio-Oil from Pyrolysis Process of Rice Husk.” doi: 10.1088/1755-1315/1097/1/012019.

Anon. n.d.-h. “MARPOL.” Retrieved May 2, 2024 (https://www.imo.org/en/KnowledgeCentre/ConferencesMeetings/Pages/Marpol.aspx).

Anon. n.d.-i. “PRAESTOL ® Cationic Polymers Municipal and Industrial Wastewater Treatment.”

Badawi, Ahmad K., Reda S. Salama, and Mohamed Mokhtar M. Mostafa. 2023. “Natural-Based Coagulants/Flocculants as Sustainable Market-Valued Products for Industrial Wastewater Treatment: A Review of Recent Developments.” *RSC Advances* 13(28):19335–55. doi: 10.1039/D3RA01999C.

Bratby, John. 2016. “Coagulation and Flocculation in Water and Wastewater Treatment.” *IWA Publishing*. Retrieved April 24, 2024 (https://ebookcentral.proquest.com/lib/aalborguniv-ebooks/detail.action?docID=4732971.).

Ciborowski Kemipol sp oo, Marek. n.d. “MOOLIWOŚCI ZASTOSOWANIA KOAGULANTU PIX W PRZERÓBCE OSADÓW ŚCIEKOWYCH.”

Fatfat, Zaynab, Mia Karam, Batoul Maatouk, Duaa Fahs, and Hala Gali-Muhtasib. 2023. “Nanoliposomes as Safe and Efficient Drug Delivery Nanovesicles.” *Advanced and Modern Approaches for Drug Delivery* 159–97. doi: 10.1016/B978-0-323-91668-4.00002-2.

Gernaey, Krist V., U. (Ulf) Jeppsson, Peter A. Vanrolleghem, John B. Copp, and International Water Association. Task Group on Benchmarking of Control Strategies for Wastewater Treatment Plants. 2017. “Benchmarking of Control Strategies for Wastewater Treatment Plants.” 142.

Gonzalez-Perez, Alfredo, Kristofer Hägg, and Fabrice Duteil. 2021. “Optimizing NOM Removal: Impact of Calcium Chloride.” 13(11). doi: 10.3390/su13116338ï.

Gul Zaman, Humaira, Lavania Baloo, Rajashekhar Pendyala, Pradeep Kumar Singa, Suhaib Umer Ilyas, and Shamsul Rahman Mohamed Kutty. 2021. “Produced Water Treatment with Conventional Adsorbents and MOF as an Alternative: A Review.” *Materials* 14(24). doi: 10.3390/MA14247607.

Hägg, Kristofer. 2015. “Calcium Chloride as a Co-Coagulant WATER TREATMENT.”

Hogg, Richard. 2012. “Bridging Flocculation by Polymers.” *KONA Powder and Particle Journal* 30:3–14. doi: 10.14356/KONA.2013005.

Ikura, Michio, Maria Stanciulescu, and Ed Hogan. 2003. “Emulsification of Pyrolysis Derived Bio-Oil in Diesel Fuel.” *Biomass and Bioenergy* 24(3):221–32. doi: 10.1016/S0961-9534(02)00131-9.

Jiang, Jia Qian. 2015. “The Role of Coagulation in Water Treatment.” *Current Opinion in Chemical Engineering* 8:36–44. doi: 10.1016/J.COCHE.2015.01.008.

Kamizela, Tomasz, Małgorzata Worwąg, and Mariusz Kowalczyk. 2023. “Environmentally Safe Method for Conditioning and Dewatering Sewage Sludge Using Iron Coagulant, Cellulose and Perlite.” *Energies 2024, Vol. 17, Page 134* 17(1):134. doi: 10.3390/EN17010134.

Kocaman, Erkin, and Meltem Yildiz. 2023. “Investigation of Starch as Flocculant for Removing Oil from Oily Wastewater.” *Journal of Water Process Engineering* 56:104499. doi: 10.1016/J.JWPE.2023.104499.

Lamanna, Leonardo, Gabriele Giacoia, Marco Friuli, Gabriella Leone, Nicola Carlucci, Fabrizio Russo, Alessandro Sannino, and Christian Demitri. 2023. “Oil-Water Emulsion Flocculation through Chitosan Desolubilization Driven by PH Variation.” *ACS Omega* 8(23):20708–13. doi: 10.1021/ACSOMEGA.3C01257/ASSET/IMAGES/LARGE/AO3C01257_0005.JPEG.

Lassen, Carsten, Steffen Foss Hansen, Kerstin Magnusson, Fredrik Norén, Nanna Isabella, Bloch Hartmann, Pernille Rehne Jensen, Torkel Gissel Nielsen, and Anna Brinch. n.d. “Title: Microplastics-Occurrence, Effects and Sources of Releases to the Environment in Denmark.”

López-Maldonado, Eduardo Alberto, Mercedes Teresita Oropeza-Guzmán, and Adrián Ochoa-Terán. 2014. “Improving the Efficiency of a Coagulation-Flocculation Wastewater Treatment of the Semiconductor Industry through Zeta Potential Measurements.” *Journal of Chemistry* 2014. doi: 10.1155/2014/969720.

MARPOL Annex I. n.d. “Annex I (Oil) OIL TANKERS OF ALL SIZES Discharging of Oil and Oily Mixtures from the Cargo Area (Including the Pump-Room).”

Nisticò, Roberto, Federico Cesano, and Francesca Garello. 2020. “Magnetic Materials and Systems: Domain Structure Visualization and Other Characterization Techniques for the Application in the Materials Science and Biomedicine.” *Inorganics* 8(1). doi: 10.3390/INORGANICS8010006.

Ofridam, Fabrice, Mohamad Tarhini, Noureddine Lebaz, E. Gagnière, Denis Mangin, Abdelhamid Elaïssari, Émilie Gagnière, and Abdelhamid Elaissari. n.d. “PH-Sensitive Polymers: Classification and Some Fine Potential Applications.” doi: 10.1002/pat.5230ï.

OSPAR Commision. 2016. “Offshore Industry Series.”

OSPAR Commission. n.d. “About | OSPAR Commission.” Retrieved May 9, 2024 (https://www.ospar.org/about).

Owodunni, Amina Adedoja, and Suzylawati Ismail. 2021a. “Revolutionary Technique for Sustainable Plant-Based Green Coagulants in Industrial Wastewater Treatment—A Review.” *Journal of Water Process Engineering* 42:102096. doi: 10.1016/J.JWPE.2021.102096.

Owodunni, Amina Adedoja, and Suzylawati Ismail. 2021b. “Revolutionary Technique for Sustainable Plant-Based Green Coagulants in Industrial Wastewater Treatment—A Review.” *Journal of Water Process Engineering* 42:102096. doi: 10.1016/J.JWPE.2021.102096.

Owodunni, Amina Adedoja, and Suzylawati Ismail. 2021c. “Revolutionary Technique for Sustainable Plant-Based Green Coagulants in Industrial Wastewater Treatment—A Review.” *Journal of Water Process Engineering* 42:102096. doi: 10.1016/J.JWPE.2021.102096.

Poologasundarampillai, Gowsihan, and Amy Nommeots-Nomm. 2017. “Materials for 3D Printing in Medicine: Metals, Polymers, Ceramics, Hydrogels.” *3D Printing in Medicine* 43–71. doi: 10.1016/B978-0-08-100717-4.00002-8.

Renault, F., B. Sancey, P. M. Badot, and G. Crini. 2009. “Chitosan for Coagulation/Flocculation Processes – An Eco-Friendly Approach.” *European Polymer Journal* 45(5):1337–48. doi: 10.1016/J.EURPOLYMJ.2008.12.027.

Rubenstein, David A., Wei Yin, and Mary D. Frame. 2015. “Mass Transport and Heat Transfer in the Microcirculation.” *Biofluid Mechanics* 267–309. doi: 10.1016/B978-0-12-800944-4.00007-X.

Scanlon, Bridget R., Robert C. Reedy, Pei Xu, Mark Engle, J. P. Nicot, David Yoxtheimer, Qian Yang, and Svetlana Ikonnikova. 2020. “Can We Beneficially Reuse Produced Water from Oil and Gas Extraction in the U.S.?” *Science of The Total Environment* 717:137085. doi: 10.1016/J.SCITOTENV.2020.137085.

Scharnberg, A. R. A., H. A. Oliveira, S. E. Weschenfelder, J. Rubio, and A. C. Azevedo. 2023. “Flocculation of Emulsified Oil-in-Water with Dodecylbenzene Sulfonate and Polyacrylamide and Floc Separation by Dissolved Air Flotation.” *Colloids and Surfaces A: Physicochemical and Engineering Aspects* 669:131496. doi: 10.1016/J.COLSURFA.2023.131496.

Shakeel, Ahmad, Ujala Farooq, and Claire Chassagne. 2020. “Interfacial and Bulk Stabilization of Oil/Water System: A Novel Synergistic Approach.” *Nanomaterials* 10(2). doi: 10.3390/NANO10020356.

Sousa, Ana M., Maria J. Pereira, and Henrique A. Matos. 2022. “Oil-in-Water and Water-in-Oil Emulsions Formation and Demulsification.” *Journal of Petroleum Science and Engineering* 210:110041. doi: 10.1016/J.PETROL.2021.110041.

Tian, Ying, Jingjing Zhou, Changqing He, Lin He, Xingang Li, and Hong Sui. 2022. “The Formation, Stabilization and Separation of Oil–Water Emulsions: A Review.” *Processes 2022, Vol. 10, Page 738* 10(4):738. doi: 10.3390/PR10040738.

Ushikubo, F. Y., and R. L. Cunha. 2014. “Stability Mechanisms of Liquid Water-in-Oil Emulsions.” *Food Hydrocolloids* 34:145–53. doi: 10.1016/J.FOODHYD.2012.11.016.

Wang, Ling Ling, Long Fei Wang, Xue Mei Ren, Xiao Dong Ye, Wen Wei Li, Shi Jie Yuan, Min Sun, Guo Ping Sheng, Han Qing Yu, and Xiang Ke Wang. 2012. “PH Dependence of Structure and Surface Properties of Microbial EPS.” *Environmental Science and Technology* 46(2):737–44. doi: 10.1021/ES203540W.

Yang, Ran, Haijiang Li, Mu Huang, Hu Yang, and Aimin Li. 2016. “A Review on Chitosan-Based Flocculants and Their Applications in Water Treatment.” *Water Research* 95:59–89. doi: 10.1016/J.WATRES.2016.02.068.

Zeta-Meter, Inc. 1993. “Everything You Want to Know about Coagulation and Flocculation.”

Zhang, Zhen, Ran Jing, Shuran He, Jin Qian, Kun Zhang, Guilin Ma, Xing Chang, Mingkuan Zhang, and Yongtao Li. 2018. “Coagulation of Low Temperature and Low Turbidity Water: Adjusting Basicity of Polyaluminum Chloride (PAC) and Using Chitosan as Coagulant Aid.” *Separation and Purification Technology* 206:131–39. doi: 10.1016/J.SEPPUR.2018.05.051.